ANKARA UNIVERSITY
GRADUATE SCHOOL OF NATURAL AND APPLIED SCIENCE

MASTER THESIS

DESIGN AND SIMULATION OF ORGAN-ON-A-CHIP SYSTEMS USED FOR IN VITRO TEST OF NANOMATERIALS

Rabia Rana DEMİRHAN

BIOMEDICAL ENGINEERING DEPARTMENT

ANKARA
2021

ÖZET

Yüksek Lisans Tezi

NANOMALZEMELERİN IN VITRO TESTİNDE KULLANILACAK BİR-ÇİP-ORGAN SİSTEMLERİNİN TASARIMI VE SİMÜLASYONU
Rabia Rana DEMİRHAN

Ankara Üniversitesi
Fen Bilimleri Üniversitesi
Biyomedikal Mühendisliği Anabilim Dalı

Danışman. Doç. Dr. Açelya YILMAZER AKTUNA

Son yirmi yılda, doku mühendisliği alanında yapılan *in vitro* hücre kültürü çalışmaları popüler bilimde geniş yer kaplamasına karşın, bazı çalışmalar gerçek doku/organı taklit etme konusunda tam anlamıyla başarılı değildir. Başarısızlığın sebeplerinden biri canlı dokuyu/organı kendi mikroçevresinden ayrı düşünürek tasarlanan sistemlerdir. Bu durumun üstesinden gelmek amacıyla son yıllarda 3-boyutlu mikroakışkan sistemler kullanılmaya başlanmıştır. Tezin amacı, henüz laboratuvar ortamında mikroakışkan çip çalışmaları yürütülmeye başlanmadan önce, o doku/organa ait hücrelerin doğal mikroçevrelerine en uygun şartların tayin edilebilmesi amacıyla gerekli tasarımın ve simülasyonun yapılmasıdır. Bu sayede, bir-çip-organ sisteminin tüm ön çalışmaları yapılmış olup, hücre davranışlarının tahmin ve taklit edilebilmesi mümkün kılınacaktır.

September 2021, 65 sayfa

Anahtar Kelimeler: Bir-çip-organ sistemi, mikroakışkan çip, comsol, simülasyon

ABSTRACT

Postgraduate Thesis

DESIGN AND SIMULATION OF ORGAN-ON-A-CHIP SYSTEMS USED FOR IN VITRO TEST OF NANOMATERIALS

Rabia Rana DEMİRHAN

Ankara University
Graduate School of Natural and Applied Sciences
Department of Biomedical Engineering

Supervisor: Assoc. Prof. Dr. Açelya Yılmazer AKTUNA

In the last two decades, *in vitro* cell culture studies in the field of Tissue Engineering have taken up a large space in popular science, but some studies are not fully successful in mimicking the real tissue / organ. One of the reasons for failure is systems designed by considering living tissue / organ separately from its own microenvironment. In order to overcome this situation, 3-Dimensional microfluidic systems have been used in recent years. The aim of the thesis is to make the necessary design and simulation in order to determine the most suitable conditions for the natural microenvironments of the cells of that tissue / organ, before the microfluidic chip studies are started to be carried out in the laboratory environment. In this way, all preliminary studies of a chip-organ system have been made, and it will be possible to predict and simulate cell behavior.

September 2021, 65 pages

Keywords: Organ-on-a-chip system, microfluidic chip, comsol, simulation

ACKNOWLEDGEMENT

I would like to express my deep and sincere gratitude to my research supervisor Assoc. Prof. Dr. Açelya YILMAZER AKTUNA, for giving me the opportunity to do research and providing unique guidance throughout this graduate thesis. Her vision and motivation have inspired me.

Nobody has been more important to me in the pursuit of this research than my family members. I extremely grateful to my parents whose love and sacrifice are with me whatever I pursue. They are magnificent role models.

Most importantly, I wish to thank my husband and also my best friend, Anıl, who provide unending support.

Rabia Rana DEMİRHAN
Ankara, September 2021

TABLE OF CONTENTS

SYMBOLS AND ABBREVIATIONS

ρ	density
ν	velocity
nm	nanometer
μm	micrometer
cP	centipoise
mol	mol
kg	kilogram

Subscripts

α	shear strain
τ	shear stress
g	gravity
t	time
wt	weight
F_D	Drag Force
C_D	Drag Force Coefficient
A	Area
2D	2 Dimensional
3D	3 Dimensional
DMEM	Dulbecco's Modified Eagle Media
ECM	Extracellular Matrix
EPA	Environmental Protection Agency
FBS	Fetal Bovine Serum
FDA	Food and Drug Administration
NP	Nanoparticle
NM	Nanomaterial
P	Pressure
PDMS	Polydimethylsiloxane
Re	Reynold’s number
RPMI	Roswell Park Memorial Institute
SA-NTs	Shear-activated Nanotherapeutics

TABLE OF FIGURES

LIST OF TABLES

1. INTRODUCTION

In recent years, *in vivo* animal and *in vitro* cell culture studies have been widely used by scientists as a reliable method in order to investigate biological processes in human and animal physiology and to create and develop treatment methods by taking advantages of several therapeutic procedures. Although these approaches are informative and will last for years, they also contain some important shortcomings (Ziółkowska, Kwapiszewski, & Brzozka, 2011).

In vivo animal studies can generate intertwined physiological responses of organs that are not possible with the use of *in vitro* conventional culture platforms. However, in these systems, it is difficult to isolate a particular tissue or cell group and to carry out physiological studies on that tissue. At the same time, in addition to ethical issues for *in vivo* modeling, there are serious biologically relevant concerns regarding association with human tissue (He et al., 2010). In current *in vitro* cell culture studies, it is possible to obtain results at the molecular level that will include the physiological responses of organs. In vitro platforms are convenient and effective for such studies. However, *in vitro* platforms often cannot simulate cell-cell and cell-matrix interactions, which are important in observing and coordinating cell behaviors and intracellular traffic (Guillouzo & Guguen-Guillouzo, 2008).

Determining the side effects of the drug composition prior to clinical investigation on humans is at the center of drug research, discove, and development studies. The cause of 4 out of every 1000 emergency room cases in the United States between 2013-2014 is the side effects of drugs on patients (Shehab et al., 2016). Due to these side effects, the number of drugs introduced to the market in the last 20 years has been gradually decreasing (DiMasi, Grabowski, & Hansen, 2016). The price of drug research, discovery, and development are quite high due to the restricted measurable of the results of in two-dimensional (2D) *in vitro* and *in vivo* studies. The current common limitations in *in vivo* and *in vitro* studies have led to the search for new systems (Ahadian et al., 2018).

In direct proportion to the increase in microfabrication studies, miniaturization, integration, and low consumption opportunities in Tissue Engineering area have increased their share in the market. Organ-on-a-chip systems allow the most accurate and precise control of many parameters. Concordantly, it is possible to imitate the complicated structures, microenvironments, and physiological and pathological responses of human organs (Wei et al., 2016).

Towards the end of the 1990s, biomicrofluidics began to gain popularity with small-scale biological applications due to the recognition of optically transparent poly (dimethylsiloxane) (PDMS) and being a soft elastomer. It is a kind of area which is mainly driven by technological developments, its main vision is to develop entire biological or chemical platforms on the surface of silicon or polymer chips. There are some crucial advantages of scaling down standard analysis setup by a factor of 1000. One obvious superiority of organ-on-a-chip systems is a dramatic reduction in required agents. Additionally, the small volumes make biological, chemical, or mechanical analyses possible to develop compact and portable systems. First, the theme of researches to obtain and analyze tissue/organ level responses against a disease by using cells of human or animal tissues/organs within microflow systems came to the fore in a study which is publishes in 2004 and covers the lung and liver systemic interaction (Viravaidya, Sin, & Shuler, 2004).

Today, most researchers use organ-on-a-chip systems effectively. For example, the US Food and Drug Administration (FDA) donated $ 5.6 million to the Wyss Institute to test organ-on-a-chip systems, which it sees as a kind of human drug studies, as are market leaders such as Emulate, TissUse, GmbH, Organovo. argues that chips will gain billions of dollars in the market soon (Organ-on-Chip Market (2016-2025), Prescient and Strategic Intelligence).

Similar to drug molecules, nanomaterials are also evaluated in detail before the clinic. Within the scope of the thesis, organ-on-a-chip system to be used for *in vitro* testing of nanomaterials will be designed. Considering the organs that affect the biodistribution of

nanomaterials in the normal physiological system, the most suitable chip material and configuration for each organ will be determined.

Simulation studies use condensed procedures of computers to test specific hypotheses and evaluate the suitability and accuracy of various methods that relate to known facts. These techniques allow studies that cannot be obtained with a single study, and that can reach precise and correct results with repetitions. Studies on simulation are increasingly used in medical literature for a wide variety of situations. Following the design, analysis of organ-on-a-chip systems will be made by taking into account parameters such as flow, pressure, temperature with flow simulation (Burton, Altman, Royston, & Holder, 2006). The design and simulation steps, which are the first steps of microfluidic chip platforms, will be carried out effectively and efficiently for our country to take its share in the aforementioned market.

2. THEORETICAL FRAMEWORK AND LITERATURE REVIEW

2.1 Microfluidics

It's known that there is not a scientific way of describing what is microfluidics because it is not at all a scientific phenomenon. So, microfluidics does not include anything from pure scientific terminology and its considerations. Basically, microfluidics is the use of devices that apply fluid flow to channels smaller than 1 millimeter in at least one size. The term deals with the behavior or controlling of the fluids (generally in sub-millimeter scale) at which surface physical characteristics dominate volumetric characteristics (Kirby, 2010).

For the better understanding microfluidics, terminology of "fluid" must be known very well. The term of 'fluid' is defined as a substance that shows continuous shear deformation in response to an applied shear force. In physics, the behaviour of the fluid is mathematically expressed in Navier Stoke's Equation which is generated from applying Newton's second law to fluid motion.

$$\rho \frac{\delta u}{\delta t} = -\nabla P + \mu \nabla^2 v + \rho g$$

where ρ = density, μ = viscosity, ν = velocity (vector), P=pressure, g = gravity.

In that equation, it's shown that fluid is affected by three main forces which are pressure gradient, viscous forces, and gravity.

Fluid mechanics are different from solid mechanics. There is a specific basic physical difference between them: While the solids become deformed under a force which is apllied on, fluid is just flow. In other words, fluids cannot to resist deformation that is caused by applied force and continue to flow as long as the force is applied.

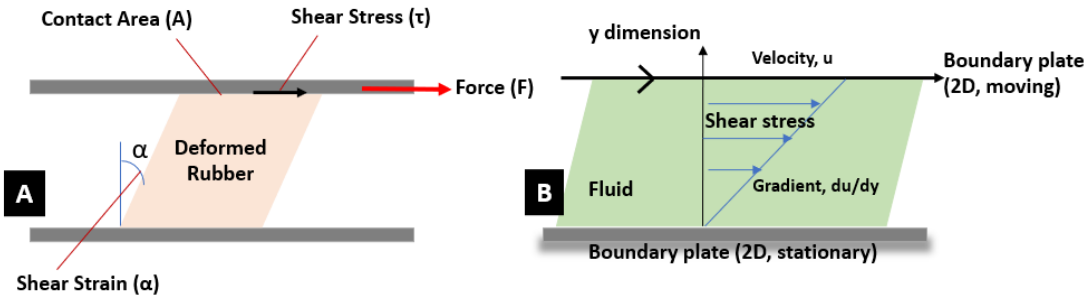

Figure 2.1 Solid state (A) Fluid state (B) shear strain under shear stress

The angle of deformation α (refers the shear strain or angular displacement) increases in directly proportional to the applied force F (Figure 2.1. A). Using the assumption that there is no slip between the plate and the rubber, while the bottom surface is in a fixed position, the upper surface is displaced in direct relation to the displacement of the plate. In figure 2.1. B, the velocity at the bottom side (boundary plate) is "0" and the velocity profile is getting large as the flow goes away from the boundary.

In solid-state shear stress applied is proportional to shear strain. The proportional factor is called the shear modulus. When equilibrium is reached solid material ceases to deform. But in the liquid phase shear stress applied is proportional to the time rate of strain. Proportional factor is called dynamic (absolute) viscosity. Equilibrium is out of the question because liquid continues to deform as long as the stress is applied.

If the fluid shows a proportional shear rate under shear stress and if it's in a cylindrical channel, the velocity profile is observed parabolic inside the channel. Fluid next to the wall have zero velocity by sticking to the wall at that point. Moving away from the wall the velocity increases to a maximum. The flow characteristic may liken the flow in a pipe. A flow gradient is observed from the surfaces of the fluids towards the centre. Under normal conditions, any part of the fluid has a different velocity than another part next to it. Particles exert forces on each other (due to intermolecular action) as a result of having different velocities between neighbour particles. If there is not a wall, the velocity gradient would not be made because of the absence of shear forces.

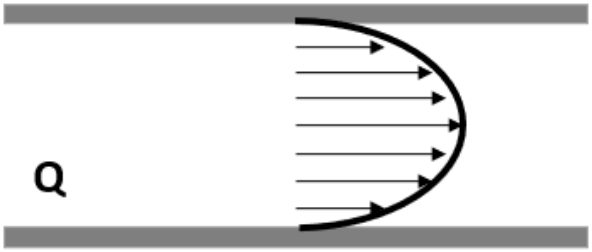

Figure 2.2 Velocity profile of fluid in a pipe

As a definiton of viscosity, it is a measure of a fluid's ability to resist gradual deformation by shear or tensile stress (Špeťuch, Petrík, Grambálová, Medveď, & Palfy, 2015).

$$\tau = \mu \frac{dv}{dy}$$

where v= fluid velocity, y= distance from solid surface, dv /dy= rate of strain, μ=dynamic viscosity, and τ= shear stress.

When the viscosity is considered as resistance to flow, velocity distribution next a boundary graph is shown below:

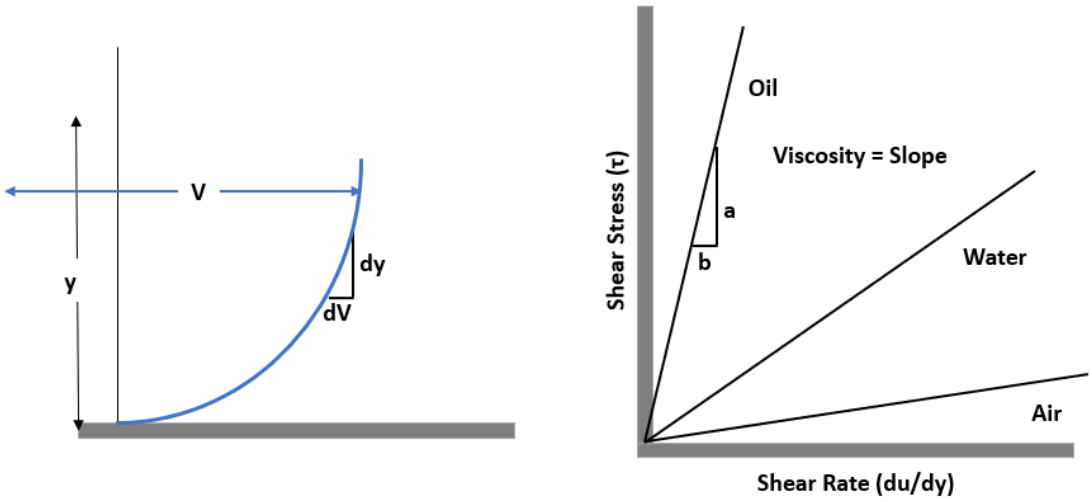

Figure 2.3 Velocity distribution next a boundary graph (Left), Viscosity graph of fluids (Right)

Viscosity, is the ratio between shear stress applied and the rate of deformation. For example, walking through a 1-m pool of water is easier than oil. Because water has less friction. Water moves out of your way at a quick rate when you applying shear stress by mean of walking through it. But oil moves out of your way more slowly when you apply the same stress.

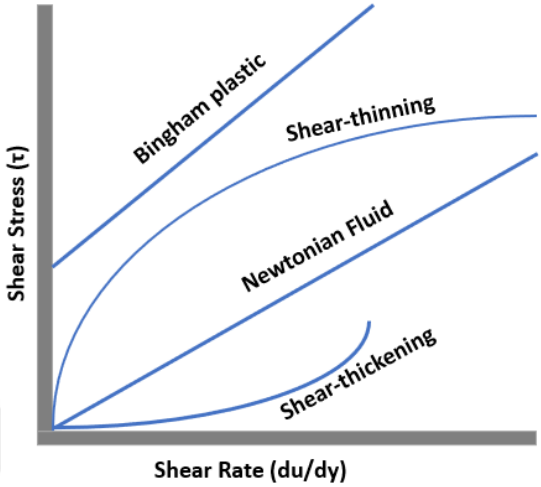

Figure 2.4 Newtonian and Non-Newtonian Fluids

The fluids are divided into two main classifications according to their behavior under shear stress next to a boundary: Newtonian and Non-Newtonian. Newtonian fluids show linearity between shear stress and shear rate on the graph. Non-Newtonian fluids are also classified as Bingham plastic, Shear-thinning, Shear-thickening, etc. Blood viscosity differs in each individual. Since the wall shear rate in venous vessels, arteries and even small vessels is much higher than 100 sec^{-1}, blood flow shows Newtonian properties near the vessel wall. However, as the vessel center is approached, the shear rate decreases and approaches zero. In the latter case, blood exhibits non-Newtonian behavior. For this reason, blood cannot be defined as a Newtonian fluid.

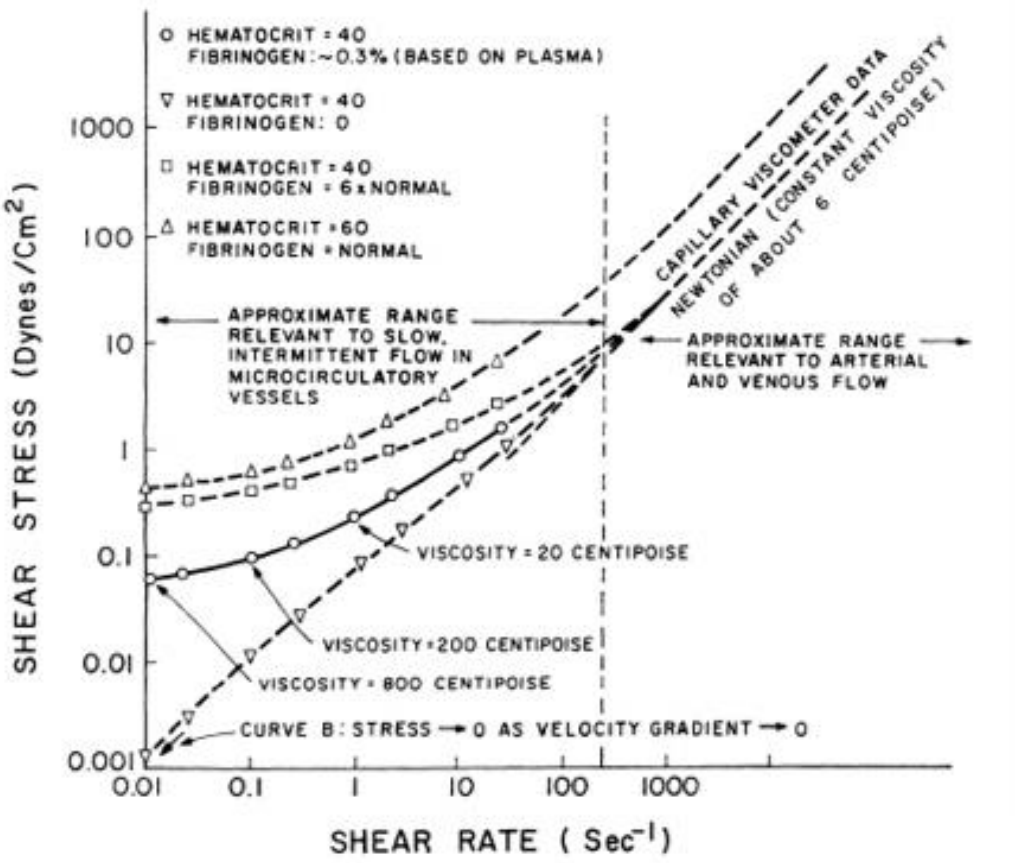

Figure 2.5 Rheology of blood (Meiselman & Merril, 1967)

The blood rheology graphs basically refers that under a shear rate of approximately 100 sec^{-1}, blood flow behaves as non-Newtonian fluid. At the same time, a quick increase in blood viscosity is observed as the shear rate decreases on this plot. When the shear rate reaches and goes up 100 sec^{-1}, the shear stress and shear rate show linearity and the blood becomes Newtonian. For these ambient conditions, there is a constant viscosity of 6 cP; however, the viscosity is measured 800 P at 0.01 sec^{-1}.

If fibrinogen, known as the coagulation protein and present at the rate of 0.3% by weight in plasma, is removed when hematocrit level is constant, at the end RBS composition may behave like Newtonian fluids. The main reason why blood shows the properity of Non-Newtonian fluid is due to the fact that fibrinogen protein is firmly attached to the RBC and acts. From another point of view, although it is known that globulin and albumin, which are other plasma proteins, affect the viscosity of the plasma, they do not provide any interpretation for the flow behavior of the blood. In addition, as stated in the

literature, serum and plasma are examples of Newtonian fluids on their own. Increasing the hematocrit means increasing the resistance of the blood to flow. The same proportion is experienced with fibrinogen concentration, as the concentration increases, the resistance of the blood to flow will increase. The basic building blocks of blood rheology are hematocrit and fibrinogen protein Concentration (Replogle, MEISELMAN, & MERRILL, 1967).

2.2 Dimensionless Reynolds Number

The physical appearance of the flow can be expressed in dimensionless numbers that represent its interaction with different factors. The Reynolds number, which is generally regarded as the most important of the dimensionless numbers, determines the flow regime and is defined as the ratio of inertia to viscous force densities (Beebe, Mensing, & Walker, 2002).

In practice, the Reynolds number formulized as below:

$$Re = \frac{\rho v d}{\mu} = \frac{F_{inertia}}{F_{viscous}}$$

where ρ = density, ν = velocity, d = diameter, μ = dynamic viscosity.

Although Navier Stokes equation describes fluid flows extensively, it was quite difficult to use on arbitrary flows where the dimensionless Reynolds number could easily categorize the fluid motion. The Reynolds number, a very important unitless number used to describe laminar flow and turbulent flow, depends on the three-dimensional image (geometry) of the flow type. For example, flow in a cylindrical capillary pipe is defined as laminar if Re<2300, transient if 2300<Re<4000, and turbulent if Re>4000. In this case, considering the fluid constant, the criterion is the diameter of the capillary tube (d) (Madrid & Toronto).

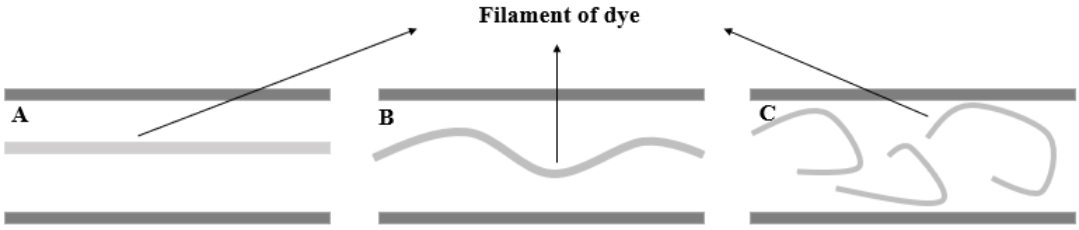

Figure 2.6 Fuid regimes: Laminar (A), Transient (B), Turbulence (C)

The Reynolds Number was first investigated by Osbourne Reynolds in the 1880s. He made a classical experiment design in fluid mechanics (Egolf & Hutter, 2020).

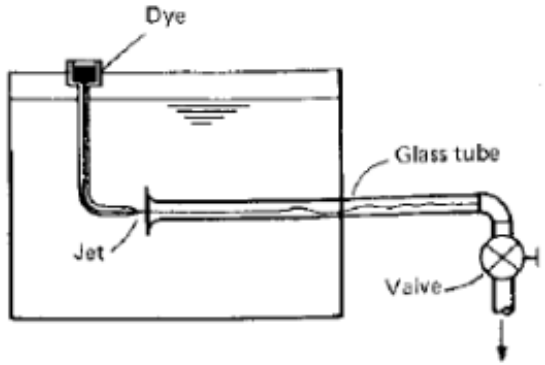

Figure 2.7 Osbourne Reynold's experiment setup (Egolf & Hutter, 2020)

In the Reynolds setup, when there was water flow in a transparent pipe, the flow lines were examined with the help of dye injected into the flow. The dye injected at low water velocities moves in the direction it was injected and there is no distortion in the flow direction. At higher water velocities, irregular movements and splashes occur in the streamline. At sufficiently high water velocities, the flow becomes completely irregular and the injected dye is distributed irregularly in the pipe. This inflow pattern is named laminar, transitional, and turbulent flow, respectively.

There is the symbolic concept of the Reynolds number: Think about a man who is running throug a hall and after a while he will pass the corner. Another man is calling behind him for turning back. It is clearly predicted that turning back would not be easy because of moment at the opposite side. At that point, the viscosity could be accepted as the desire to adhere to the wall. What should be expect at the end? The running man is pulled toward

the wall. Re is considered decrea, or the viscosity increase; he can turn corner as much as possible. Considering that Reynolds number is low, you might think that you would run adjacent to the wall (laminar flow); if the Re number is high, when you reach the corner you will break away (turbulent flow).

In a laminar flow regime, layers slide over each other like playing cards, and the dye does not mix with water. The mathematical analysis is partially easier at that regime. Turbulence occurs at higher speeds, resulting in eddies. So, the dye mixes rapidly and completely. The turbulent flow regime cannot be realized by the naked eye. The detection of irregulated flows are very hard to notice so, the laser must be used. Viscous forces are forceful in laminar flow and inertia forces are more active in a turbulent flow.

If you deal with a microchannel, the numerator of the Reynolds number which is inertia forces is too small due to low dimensions of the channel, while the denominator which is viscous forces usually states constantly for most fluids that relevant to Newtonian fluids. So, it's mean that the velocity is the main consideration which is the flow whether turbulent or not.

2.3 Traditional Tissue Engineering Platforms

In 1993, Langer and Vacanti defined Tissue Engineering as a multidiscipliner field that focus on engineering and biology in order to sustain, restore, or develop the functional features for damaged tissue (Langer & Vacanti, 1993; Lanza, Langer, Vacanti, & Atala, 2020). The basis of tissue engineering is improve tissue regeneration process and so to eliminate all kinds of inconveniences that may occur during organ transplantation such as graft versus host diseases. Scientists have recently used *in vivo* and *in vitro* platforms to discover biological processes in human and animal physiology and to create and develop treatment methods by taking advantages of several therapeutic procedures.

Understanding of how the cells and microenvironments are interact each other is not an easy issue. As the human body at cellular level improves, the accumulation of the knowledge about interactions significantly increases. It's known that the knowledge must

be utilized in the development of new therapies for diseases and drugs for those treatments.

In order to mimic unknown drug or therapeutic chemical effects on original tissue the *in vivo* platforms or in other words animal testings are setup. The method basically involves that the chemical ingredient such as drug is introduced as input through the body fluid of animal and the outputs such as concentration gradient, chemical observations are evaluated by taking samples from the animal body fluid. Although, the outputs can be examined in every aspects, it is difficult to learn how the internal proceedings occur in mainstream. Besides, the animal cells are different in size, contents, lifetime, physiology, and metabolism from humans'. That is caused lack of confidence of the animal *in vivo* tests in transition from preclinical to clinical studies (Stirland, Nichols, Miura, & Bae, 2013). More importantly, the ethical issues of *in vivo* platforms have been argued. According to 3Rs principle (Replacement, Reduction, and Refinement) of Russel et.al. carrying on an *in vivo* study creates national and international legislations. Before *in vivo* analysis, both getting ethical committee approval and disposal of animals are time consuming parts for evaluation drugs (Russell & Burch, 1959).

In order to overcome the shortcomings of *in vivo* platforms, *in vitro* studies which is culturing the natural human cells outside of the body/on a flask has been developed. At first stage, the *in vitro* platforms were structured in two-dimension mold. The cells are cultures as monolayer on the platform. Then, the drugs or chemicals are added on the cells. After a while the cellular response are noted sistematically. As a result, signals which is come from cells examined in detail. *In vitro* studies has an advantage of screening the drug mechanism of action with the help of different imaging techniques. However, at that point it is almost impossible to constitute cellular microenvironment. Cell-cell or cell-extracellular matrix interactions cannot be mimic on *in vitro* studies (Bhise et al., 2010).

Under favour of technological claims which is resultant from mimicking three-dimensional (3D) natural environment in humans, it has forced the creation of simplification ECM. 3D cell culturing platforms are designed commonly as spheroids

(Llewellyn et al., 2020) and cell sheets (Kimlin, Kassis, & Virador, 2013). Basically spheroids are formed clusters of significant cells which are also suspended in an appropriate culture medium. Those group of cells are comprised by hanging drop technique which are most similar to *in vivo* environment by means of functionally and physically. In Tissue Engineering generally the tumor studies are carried out by forming spehorid cultures (Drewitz et al., 2011; Fennema, Rivron, Rouwkema, van Blitterswijk, & De Boer, 2013; Llewellyn et al., 2020). Cell sheet techniques involves a cell layer culturing onto the temperature-responsive culture dishes. While the cells are adhered to the bottom of the dish at 37 °C, they can be detached easily by reducing the temperature to 27 °C. Addidng one cell sheet to the another, the 3D culturing model is formed. By taking advantages of the cell sheet technique, the cornea (Burillon et al., 2012), cardiac (Sekiya et al., 2009), or muscle tissue repairs are experienced.

Though, 3D *in vitro* platforms has seemed remarkebly better opportunuties over *in vivo* platforms, excessive the cellular aggregation on multilayer culture sheets may cause accumulation and finally death of the cells. Moreover, providing 3D environment to the cells does not meet the same meaning of exact cellular reaction by means of electrical or mechanical responses. For example, during inhalation procedure, the volume of the lungs changes instantly and so the lungs cells are exposed large amount of mechanical stress. Besides, the surface-area-to-volume ratio increases at that point. It affects the carbondioxide and oxygen exchange parameters. The mechanical criterias on cellular behavior has same importance with chemical responses. From the point of view, 3D *in vitro* platforms has owing insuffiicient essential cellular behaviours (Wang, Samanipour, Koo, & Kim, 2015).

2.4 Overview of Nanomaterials & Applications

A nanometer (nm) is decribed as an International System of Units (SI) that refers 10^{-9} meter in length. A nanomaterial is commonly introduced to be of diameter in the range of 1 to 100 nm in principle. There are different opinions in defining nanomaterials (NMs). For example, according to Environmental Protection Agency (EPA), “NMs can exhibit

unique properties dissimilar than the equivalent chemical compound in a larger dimension" (Jeevanandam, Barhoum, Chan, Dufresne, & Danquah, 2018).

Bulk materials can have several physical attributes regardless of their size, however at nanoscale, the attributes are usually show differences according to their shape and size. Besides, the ratio of surface area to volume determines the physical, chemical, bological properties of NMs (Demir, 2021). There are many different shape and size format of NMs as shown on figure 2.8. What makes nanotechnology so interesting is that materials behave differently from the macro world in this dimension. For instance, while carbon is a kind of element which is used for fuel in coal, or for printers in making ink; the carbon nanotubes are frequently used in implant materials because of their robust and flexible structures. The earlies 2010s the studies of NMs are began to reach top. With the increase demands of nanomaterial studies, "The Nanotechnology and Nanomaterials Global Market Report 2020" predicts the manufacture of nanomaterials approximately 22.000 tones (Inshakova, Inshakova, & Goncharov, 2020).

The nanomaterials have perfect reactivity in bio/chemical reaction by virtue of their high surface-to-volume ratio. Additionally, modfying nanomaterials with several methods by encapsulating or binding to other materials. For instance, some antibodies can easily be linked with nanomaterials to catch specific biomarkers in order to imaging or detection. Morever, NMs possess some inherent properties e.g. magnetic resonance for magnetic particles. Furthermore, owing to ability of NMs to develop the quality of material features and behavior involving the flexibility, durableness, and performance are acceleratingly used in industrial facilities (Mahto et al., 2015). The several surface functionalizations facilitates biomedical applications such as detecting, tagerting, imaging, drug delivery, and therapy which are also trend scientific issues nowadays.

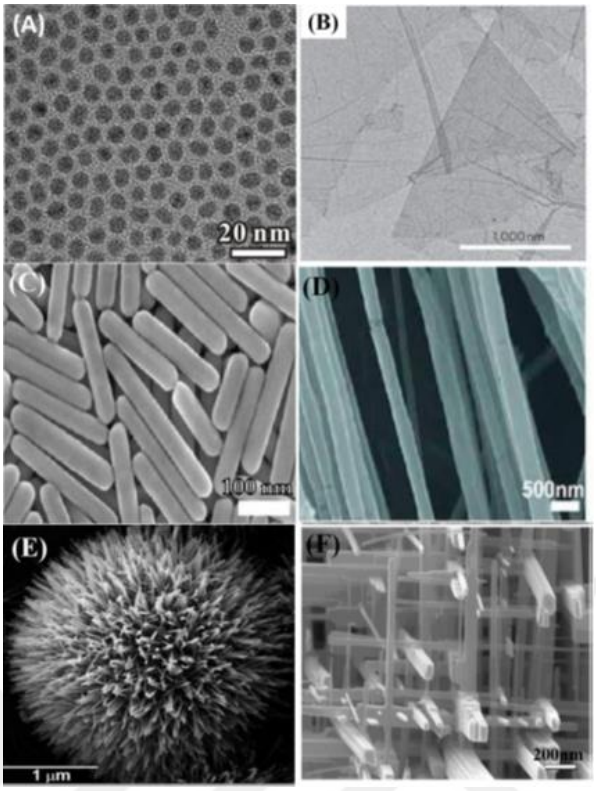

Figure 2.8 Nanomaterials in different morphologies. (A) nonporous; (B) nanosheet; (C) nanorods; (D) nanofiber; (E) nanowire; (F) nanowire network (Mahto,2015)

NMs can be integrated to biosensors which allows more precise, sensitive, and rapid detections. They are also minimize amount of biomarkers. Furthermore, the NMs can move inside the body easily, so that they can reach almost everywhere in the body via the blood vessel. This approach is fit to the therapeutic effect of NMs as controlled drug delivery (Hernández-Pedro et al., 2013).

Nanomaterial safety strategies are mainly involved *in vitro* and *in vivo* approaches. Up until now, before the introduction of NMs to body fluid the animal tests are applied. But, insufficient correlation between the animal models and human trials because of the genetic factors cause defaults. Additionally, low concentration for long-term observations does not applied on in vivo platforms. Those kind of studies are generally ended up acute toxicity observations. Ethical issues and time consuming problems should also be considered.

In vitro studies are inadequate and shallow as in vivo studies though they have gaining popularity in recent 20 years for NM toxicity. However in vitro models are optimized in conventional one-dimensional non-flow cultures, whereas flow which is like actual clinical effects will produce coser results to normal physiology. It must be noted that the control of exposure NMs to cells are also not as much as possible. The most important problem is aggregation of NMs (Oddo et al., 2021; Tiwari & Tiwari, 2020).

2.5 Microfluidic Devices

To overcome shortcomings of both *in vivo* and *in vitro* platforms, microfluidic devices have been developed in last three decades by taking inspiration of microfluidic systems. The most important advantage of microfluidic systems over traditional methods, which will be discussed the others in detail in the following sections, is able to create a dynamic cell culture environment for Tissue Engineering applications such as developing therapeutic strategies, laboratory testing methods, etc.

The first generation of microfluidic device materials were silicone or glass. After a while, it was realized that because of their high thermoconductive property, the microprocessing of glass were found expensive and time-consuming (Xiong et al., 2014). With the discover of poly(dimethylsiloxane) (PDMS) which is optically clear, flexible, and biocompatible material the microfluidic devices are began to used in biological process (Duffy, McDonald, Schueller, & Whitesides, 1998; Xia & Whitesides, 1998). The manufacturing technique of PDMS fabrication is shown the figure below:

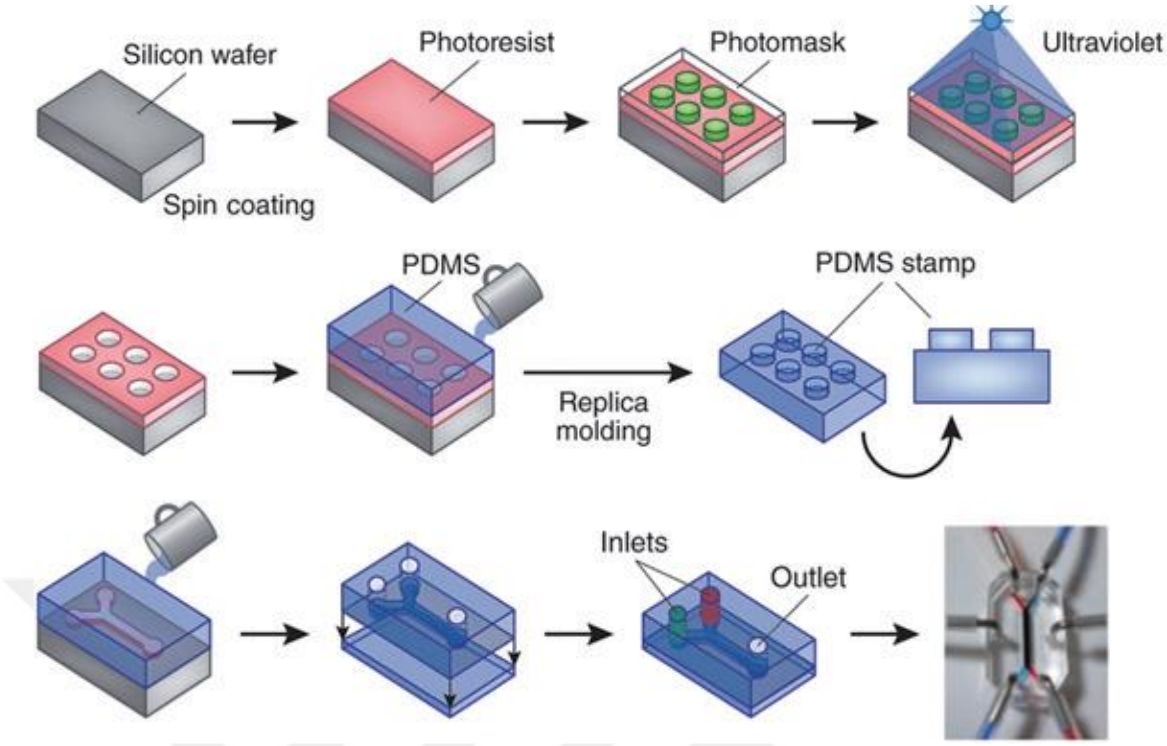

Figure 2.9 PDMS Microfluidic chip manufacturing process (Wang et al., 2015)

First, the silicone layer is coated via photoresist material. Then, photomask material is used for limit the photoresist layer crosslinking under exposure of UV light. After that the pattern becomes a mold for PDMS. The PDMS is poured on the mold, then it is waiting in an oven to polymerize. The soft litography technique can be used also for microchannels on PDMS structure to permit fluid flow inside it (Wang et al., 2015).

The first concept of biomicrofluidic chip design was introduced in 2004 when Michael Shuler and his colleagues published on liver and lungs interaction study. Essentially, they mimic the circulatory system and chambers in an organ-on-a-chip system to predict responses of liver and lungs by introducing chemical component (naphtalene as a toxicant) from the inlet of the chip (Viravaidya et al., 2004).

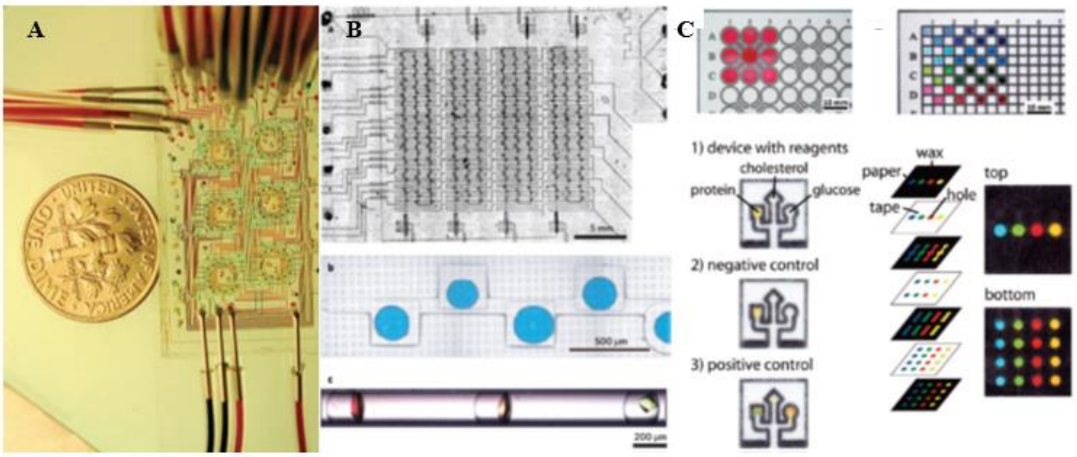

Figure 2.10 Microfluidic biorector design (Balagadde et al., 2005), Droplet based micrfluidic chip (Zheng et al., 2004), Paper based microfluidic chip (Carrilho et al., 2009)

One of the most important advantages of the microfluidic systems is their transparental shape. Besides, because of the low dimensions of channels inside the microfluidic chips, the fluid regime must be laminar. The features providee the precise control of supplies and waste as shown figure 2.10 (A). Frederick and his colleagues designed a microfluidic bioreactor network to avoid biofilm formation. Six independennt bioreactor, and several microchannels were easily observed under optical microscopy by real-time measurement of cell morphology (Balagaddé, You, Hansen, Arnold, & Quake, 2005). Another significant advantage of the chips is the usage minimum sample, chemicals, cell, and/or culture media. In figure 2.10 (B), the scientiest studied on droplet based micrfoluidic system to keep under control evaporation of water by using nanoliter droplets (Zheng, Tice, Roach, & Ismagilov, 2004). When the term of "device" is handled, it can be thougt as cost systems. However, if you deal with diagnostics on mirofluidics chip, it may be cost almost $0.001 per device. From that point of view, the microfluidic chips are cost-effective and easy to design as shown in figure 2.10 (C) (Carrilho, Martinez, & Whitesides, 2009).

An organ-on-a-chip design commonly is consist of micro-sized channels, wells, and different types of membranes in order to make it possible *in vivo* like *in vitro* system. The field of organ-on-a-chip has been developed by the helping of advance technologies, then it grows newly generated microfluidics platforms such as blood vessels, liver, lung, lymphatic system, gut, muscle, etc. (Zhang, Korolj, Lai, & Radisic, 2018).

Liver is one of our vital organ which is responsible for detoxification, blood filtering, etc. Liver-on-a-chip systems are primarily used for better understanding of drug metabolism (Knowlton & Tasoglu, 2016; S.-A. Lee, Kang, Ju, Kim, & Lee, 2013; Theobald et al., 2018). In liver-on-a-chip systems, there are three subsections which are hepatocytic cells included main field, an endothelial barrier, and a circulatory channel for nutrient flow. The sections are designed mechanically according to the aim of the study. For example, if the nutrient flow is placed outside of the microfluidic chip, it can be operated for transportation of blood and measurement shear stress over hepatocytes when the blood flows through channel (P. J. Lee, Hung, & Lee, 2007).

In FDA database, it is saved that there have been a limited approval of nanomaterials which are used for drugs. Fort his reason it is definitely necessary to improve testing platform to confirm the therapeutic efficacy of drugs/chemicals to avoid adverse effects on humans. Kwak et al. developed a microdevice to study interaction between the drug and tumor cell by mimicking lymphatic, capillary, and tumor channels. Forming natural tumor microenvironment made as much as easy the determination of complex transport of drugs through the channels and porous membranes (Kwak, Ozcelikkale, Shin, Park, & Han, 2014).

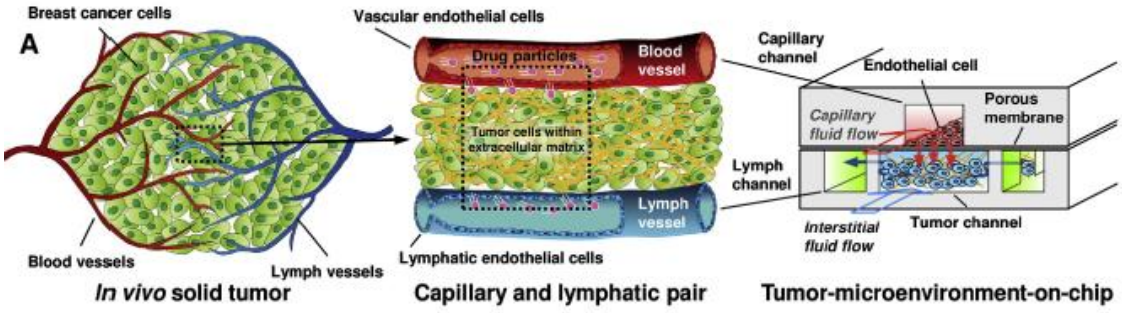

Figure 2.11 Tumor microenvironment on a chip design (Kwak et al., 2014)

The most important items in the establishment of existing organ-on-a-chip systems are determination the physiology of the organ to be designed, physical and mechanical design according to the intended use, simulation and analysis of the designed chip. In this context, organ physiology, cell types in the organ, cell-cell interactions, cell-ECM

interactions should be evaluated. Another factor affecting the evaluation result is the blood flow to which the cells are exposed. All the factors mentioned above will give us clear information about the microenvironment of that organ. When organ physiology is thematically completed, appropriate mechanical design should be done. The material to be used in making the microfluidic chip is determined and the path on which the flow should follow is drawn. The simulation phase can be defined as the last step before the organ-on-a-chip systems are put into use. In that process, it is benefited from microfluidics terminologies.

In the present study, it is aimed that, before starting mcrofluidic chip studies in the laboratory environment, the necessary design and simulation are made in order to determine the most appropriate conditions for the natural microenvironments of the cells of that tissue / organ. In this way, all preliminary studies of one-chip organ system have been made, and it will be possible to predict and simulate cell behavior.

3. MATERIALS AND METHODS

In the present study, a computer 'CAD' based drawing program and a computer software that allows microflow simulation was used as research material. One of the most common programs used for 2-3D design purposes in the literature is SolidWorks and the other is AutoCAD, but SolidWorks was preferred in this study due to the ability to use it. Currently, a wide variety of simulation programs are used in the market. The most common of these is ANSYS, and COMSOL Multiphysics software has been preferred due to some advantages over ANSYS. Both are software that are capable of solving multiphysics problems in the designed model and purpose. However, since microflow systems was imitated on the design, all simulations was carried out on the "Microfluidics" module on the COMSOL Multiphysics software.

3.1 Organ Physiology to Be Designed

Before starting a organ-on-a-chip design, the organ should be well known. The region where the organ is located, the rate it receives from the cardiac output, what type of cells it consists of, and its interaction with the cells in its microenvironment are the main factors to be considered. In the present study the organs that were discussed below were chosen to evaluate in every aspects including their physiology and anatomy.

3.2.1 Vessel-on-a-Chip

Blood vessels are like a network which is in charge of transporting blood through all over the body. It’s known that blood is moved where the pressure is lower than the region of high pressure flowing into the area. As with all liquids in the universe, it is in principle that under a certain pressure difference, blood will flow from where the pressure is high to where it is lower. There is no direct contact of blood with cells. Interstitial fluid is located in the capillaries to allow the passage of substances between the blood and cells. Nanoparticles or chemicals are transported inside blood vessels and diffuse between blood and tissues with the help of interstitial fluid.

Blood vessels were designed in the present study for simulating the main and capillary channels. Shear stress which was applied on the vall of the vessels was observed.

3.2.2 Liver-on-a-Chip

The liver is the largest organ in the body where many different functions are performed and at the same time, these functions are connected to each other. The liver weight in an adult is approximately 1,5 kg. The functional unit of the liver is called the liver lobule, of which is cylindrical in shape. Liver lobules are composed of structures around a central vein. These central veins drain into hepatic veins and into them vena cava. Liver lobules made of hepatic cellular plaques are in the form of rods extending from the inner central vein to the outside. The lobule itself is composed principally of many liver cellular plates. There is small bile canaliculi between the cellular plates .

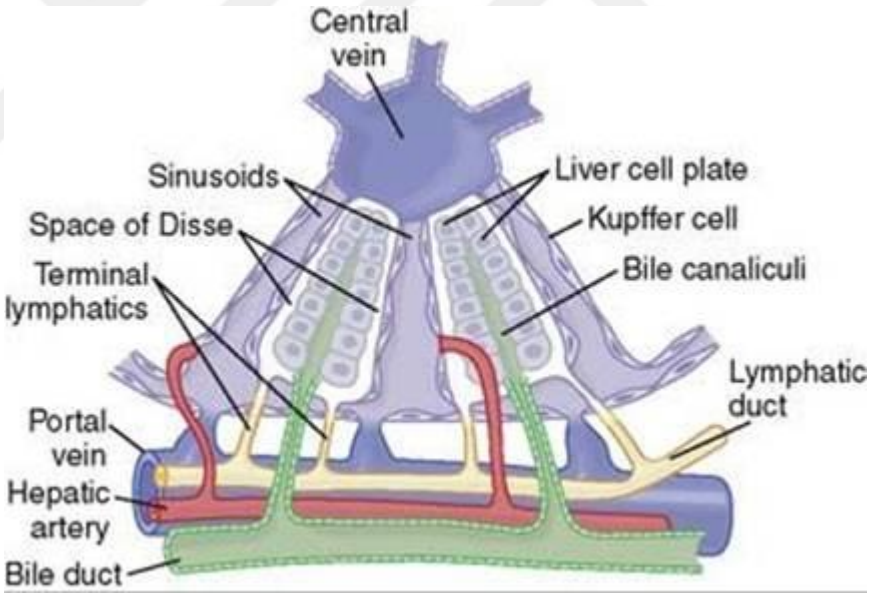

Figure 3.1 Liver functional unit (Guyton, Taylor, & Granger, 1975)

Blood flows into the portal veins from the gastrointestinal tract into the small portal venules between the compartments, then into the hepatic sinusoids extending between the hepatic plates, and finally into the central vein. The blood coming from the hepatic artery is poured into the hepatic arterioles between the divisions, then directly to the hepatic sinusoids and finally to the central vein. Blood coming out of the liver is poured into the

hepatic vein into the vena cava. The pores in the hepatic sinusoids are very permeable, allowing both liquid and proteins to easily pass into the Disse gaps, thus, excess fluid in the liver can be removed by lymphatic channels. The main functions of the liver are blood storage, blood purification, metabolic functions and detoxification (Kalra, Yetiskul, Wehrle, & Tuma, 2020). Detoxification is the conversion of bioactive substances such as hormones, drugs to less toxic. It is formed as a result of chemical transformation and metabolic activities. Nanoparticles, which may be used as drugs, diagnostic chemicals, etc. is metabolised in liver.

In the present study, the liver-on-a-chip design was determined as three section system which capable of introducing drug/nanoparticle and cell seeding parts.

3.2.3 Tumor-on-a-Chip

The main purpose in cancer research is to closely observe metastasis and understand the relevant tumor biology so that anticancer drugs and treatment approaches can be developed. The tumoral spheroids reflect the three-dimensional growth and organization of solid tumors in a very realistic way, and as a result, they can more clearly reveal the intercellular relationships and microenvironmental conditions in tumors. At the same time, there may be different drug response between the findings obtained in two-dimensional *in vitro* tumor spheroid applications and the findings obtained in the clinic.

Tumor spheroids are usually created by self-assembly. The most common technical methods are pellet culture, hanging drop, rotating wall vessel, and magnetic levitation (Ryu, Lee, & Park, 2019). The hanging drop method is a well-established method and is more suitable for creating a microenvironmental niche. First, as a general method, it is begun from a monolayer cell culture, then to obtain desired cell density the suspension is diluted with fresh medium. After that, the prepared cell suspension is dispensed into as small drops the petri dish by the helping of pipette. A cap is placed on the petri dish and the entire petri dish is turned down. The drops of cell suspension attached on the top of petri dish thanks to simultaneous action of surface tension and gravitional force (Wan, Neumann, & LeDuc, 2020).

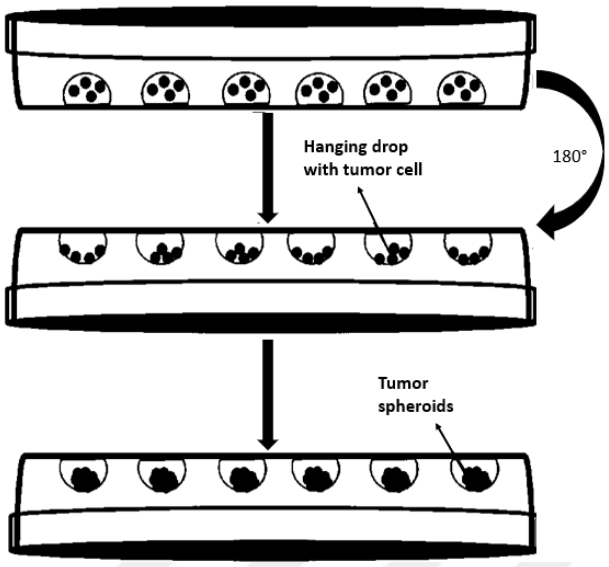

Figure 3.2 Tumor Spheroid Method (Hanging Drop Technique)

The tumor spheroids desin was chosen fort that study to make the most effective design to observe the metabolism of drug/nanoparticle-containing substances on tumor-on-a-chip systems by considering the mechanical and shear forces which affect the cells in their natural microenvironments.

3.3 Technical Drawing and Configuration

SolidWorks® is a CAD software used to create 2D and 3D solid models simply, quickly and effectively. Like other CAD programs, it is specialized in accordance with the original goals of practice, creating a distinctive ecosystem. However, it has some superiorities from other CAD programs such as accesibleness, easy to use, etc. SolidWorks, which has been continuously developed since 1995 and reached a large user base, is basically the first 3D modeling program that works with Windows operating systems.

Designing a technical drawing the workflow is listed below:

1- Creating a new part by selecting workspace such as front plane, right plane etc.
2- Sketching a reference line to the center of your sketch
3- Drawing the conceived 2D part by taking guide the center line

4- Creating 3D body of the design by using “Extruded Base Command”
5- Postprocessing the design
6- Save the ‘cad’ file as ‘dxf’ format in order to import it to COMSOL software.

Thecnical drawings of organ-on-a-chip systems which involves platforms, channels, etc. were done by using SolidWorks® program. It can also communicate with COMSOL® by the helping of its extension.

3.4 Simulation

COMSOL Multiphysics® is a kind of simulation environment designed with real world applications in mind. The determined goal of the whole simulation is to mimic as much as possible the effects actually observed. They must be in an engineering or scientific context. Multiple physiology is needed to achieve this.

COMSOL includes scientific models which are acoustic, electromagnetic, chemical reactions, mechanics, fluid flow and heat transfer. It allows traditional physics-based user solutions and bound systems of differential equations.

Basically, COMSOL Multiphysics studies were executed by following the steps below:

1- Setting up to model environment from “Model Wizard” or “Blank Model” section. (In the present study model wizard was used to import dxf file of SolidWorks mechanical design to COMSOL.)
2- Selecting space dimension such as 3D, 2D, etc.
3- Selecting the physics such as fluid flow, heat transfer, etc. It can be a single physics or combination of multiple physics.
4- Selecting a study based on the physics in the model such as stationary, time dependent, etc.
5- Adjusting “Model builder window” parameters:
   - Creating definitions (parameters, variables, functions)
   - Importing/Creating geometry
   - Adding material from library or defining the material properties by hand

- Defining the physics that was chosen before
- Examining the mesh options such as coarser, extra coarser, etc.
- Running the simulation
- Postprocessing the results

In this project, the organ-on-a-chip systems that were drawn in SolidWorks® were integrated into the COMSOL Multiphysics simulation program. The ‘cad’ files were imported for simulation. At the beginning of the simulation, simple 2D flow simulations were performed. All simulations were performed on Microfluidics module of the program. After that, the material selection was done in accordance with the type of organ-on-a-chip. When the appropriate material selection was done, the fluid type and its flow characteristics was determined with respect to natural microenvironment of organs, the culture media which is generally used *in vitro* platforms.

4. RESULTS

Following the working methodology of the project previously mentioned technical drawing of organ-on-a-chip systems and their simulations on COMSOL Multiphysics were evaluated below.

4.1 Vessel-on-a-Chip Design

4.1.1 Branched vessel modeling

In SolidWorks the 2D model of vessel-on-a-chip was designed. The biggest main channel has 20 µm diameter, was divided two channels and then those two channels were also divided two each other. Finally, four channels were obtained as a vascularization branching with a diameter of 15 µm. The total length of the vessel-on-a-chip is 360 µm.

Two different design that are same entirely except corners were drawn. One of them was adjusted sharp and other has soft edges in order to analyse shear stress on the boundaries. The following analyses were run on sharp edged vessel-on-a-chip design.

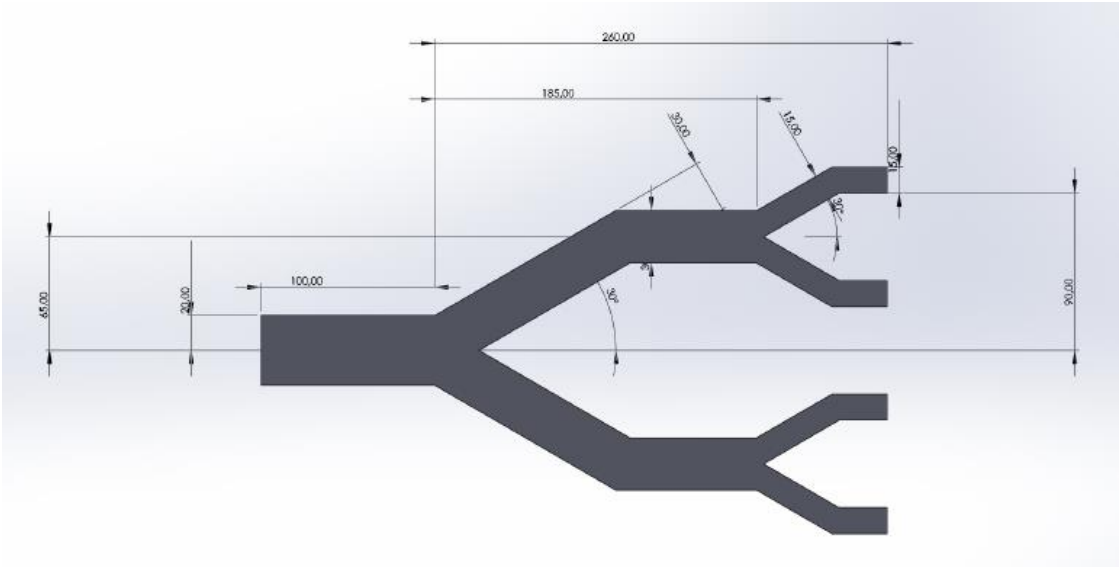

Figure 4.1 Technical Drawing of Branched Vessel Modeling

Then, the “Model Wizard” window was chosen. 2D space domain was selected to get ready to transfer the technical drawing from SolidWorks. The 2D presentation of vessel-on-a-chip was performed using “Geometry” tools by exporting the model (Figure 4.2). Because of the working on microfluidic chips, length unit was selected as “µm”.

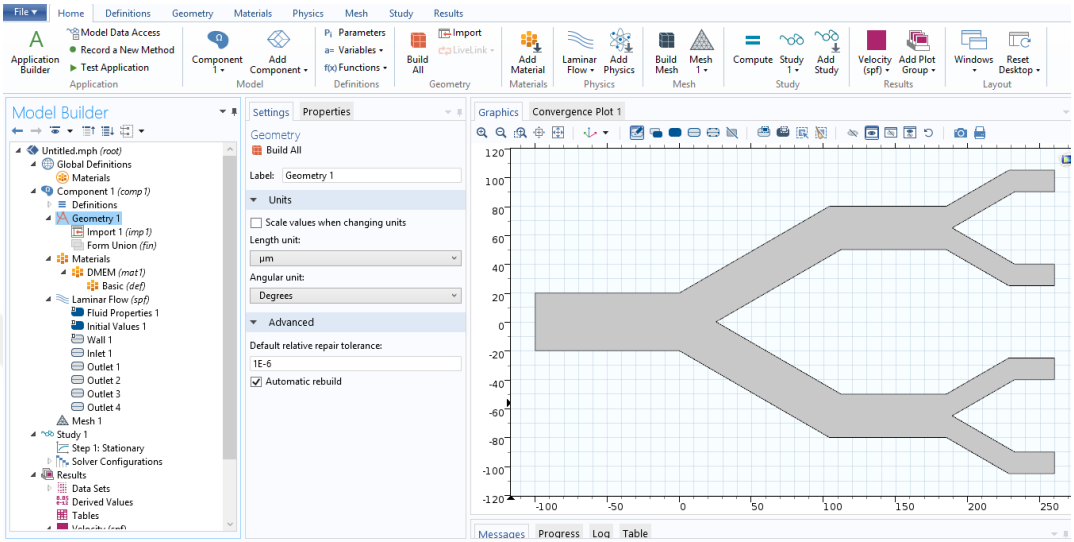

Figure 4.2 Importing Geometry on Comsol

The material selecton was done by using “Materials” tools. Water was found from the library of COMSOL. After that, the Physics which is “Fluid/Single-Phase Flow/Laminar Flow” was added. In order to evaluate steady state fluid flow “Preset Studies/Stationary” was chosen. For the material which will flow through the microfluidic chip was set by selecting “Blank Material” first. Then, in order to simulate DMEM (Dulbecco’s Modified Eagle Medium), which is a kind of common culture medium for cells, was planned to simulate. Known properties of DMEM (dynamic viscosity and density) was added to blank material. Dynamic viscosity and density of DMEM are 0.89 mPa.s and 997.04 kg/m^3 respectively.

Inlet and outlets were assigned as the largest channel being inflow and the others being outflow channels. After that, the triangular meshes were generated in the vessel-on-a-chip geometry of the present study. The simulation was began from “Study1” to evaluate steady state flow. (Figure 4.3)

It was recorded that the increase in cross-sectional area that results in a decrease of velocity (flow continuity equation). While the maximum velocity is 0.075 m/s on main channel which has 40 µm diameter, on subchannel which has 30 µm diameter maximum velocity is 0.055 m/s. The pressure values as recorded maximum $3x10^8$ Pa minimum $0.06x10^8$ Pa.

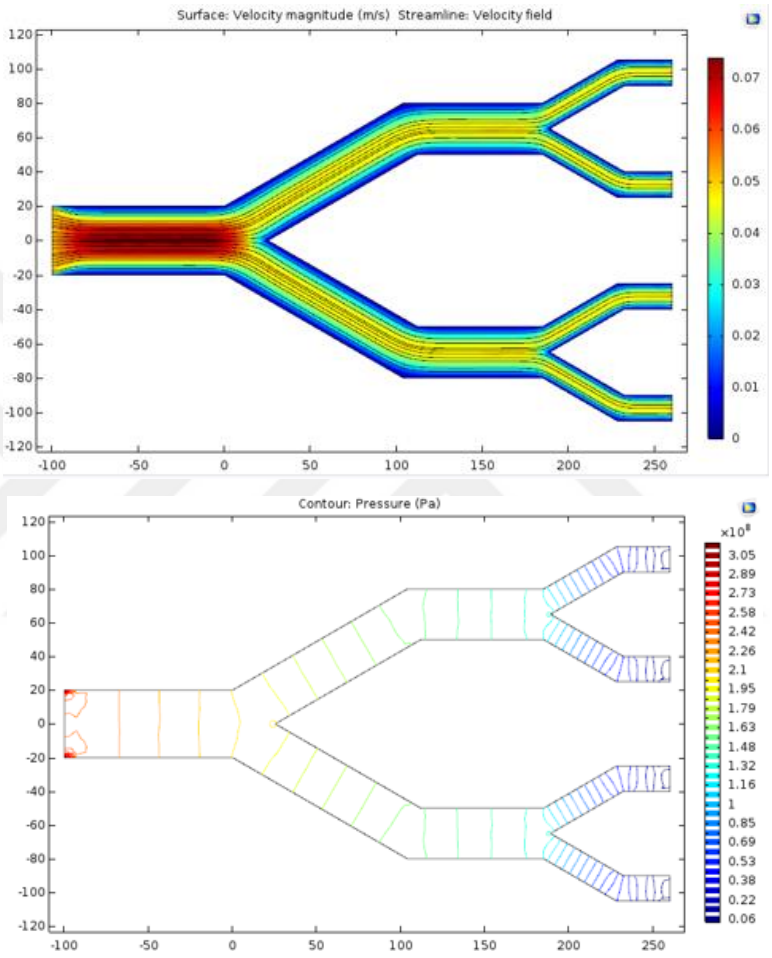

Figure 4.3 Velocity Profile of Fluid on Branched Vessel Modeling (above) Pressure Profile of Fluid on Branched Vessel Modeling (below)

4.1.2 Microvascular occlusion on chip

The microvascular occlusion modeling was drawn by getting inspired from normal vascular blackage disease. Technical drawing (below) consist of one main and two subchannels which divides from main channel. Main channel has 200 µm diameter. Bigger channel which was divided from main channel has 300 µm diameter and the

smaller channel has 100 µm diameter. First, the laminar fuid flow analysis was carried out on normal vascular formation. Then, occlusion modeling was done on bigger channel walls by changing the geometry and narrowed size of the obstructed part.

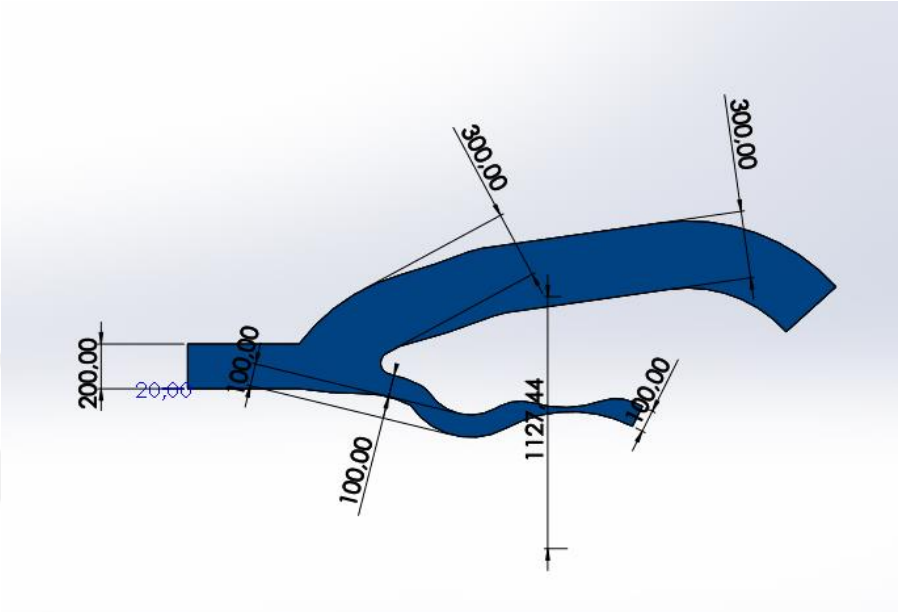

Figure 4.4 Technical Drawing of Vascular Occlusion

The blockage of vessel modeling was applied four different mechanism. For the beginning one side blockage was applied by narrowing the channel with 500 µm diameter of a semicircle. The narrowed length was decreased from 300 µm to 166 µm. After that, both side blockage was applied with the same diameter circle obsturction and same narrowed length.

Mesh of the microfluidic chip was applied “Physics Controlled” that has more triangular shapes near boundaries for simulating laminar fluid flow characteristics on every piece of chips. Inlet of the device was introduced on main channel ant subchannels have outlets. Inflow velocity measurement was adjusted 0.05 m/s and studied in staionary. Those properties were kept same for all four different simulations. It was aimed that analyzing the possible differences between one and two side obstructions on microvessels in first two statioary studies and resulted as below.

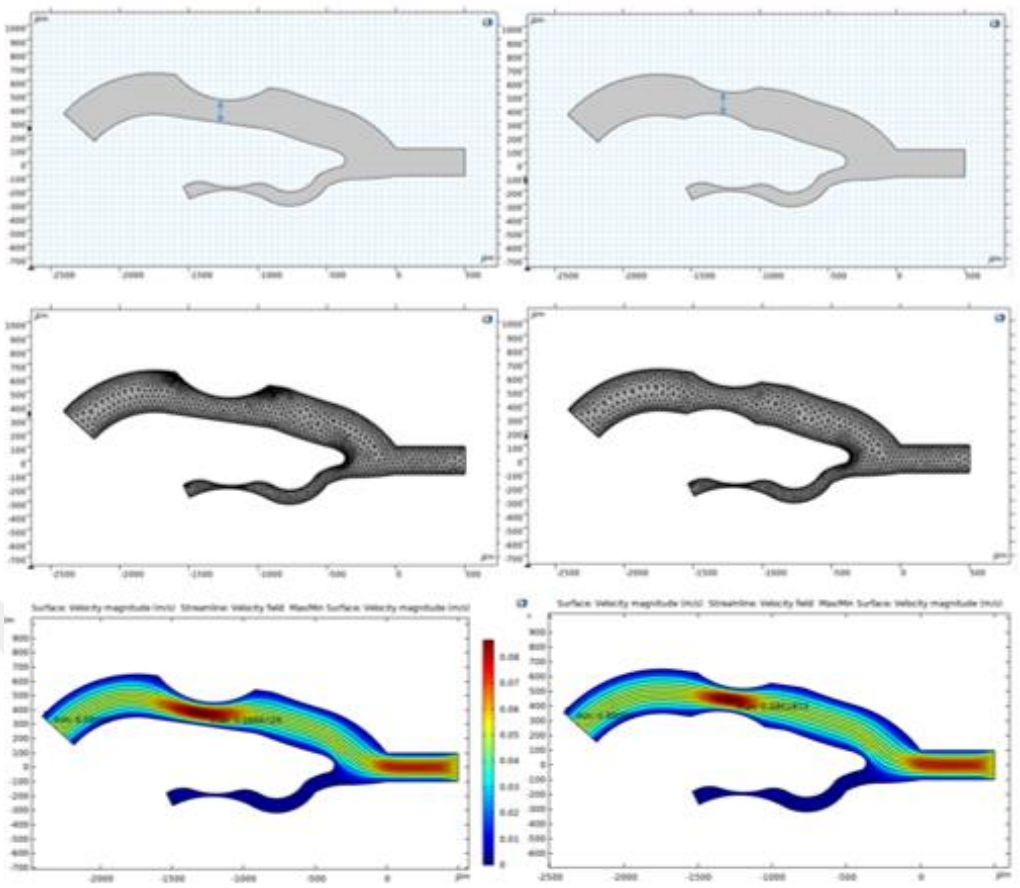

Figure 4.5 Single (Left) and Double (Right) Side Occlusion Simulation Process

As shown in the figure 4.6 both single side and double side of occlusion has maximum velocity of 0.086 m/s at the middle part of the obstruction and minimum velocity of 0 m/s on boundaries because of no-slip of conditions. However although the maximum and minimum velocity measures are same in both single and double side obstructed design, velocity contour is much intensive single sided caused occlusion. On double side obstucted vessel modeling the rate of the increase and decrease of velocity is high.

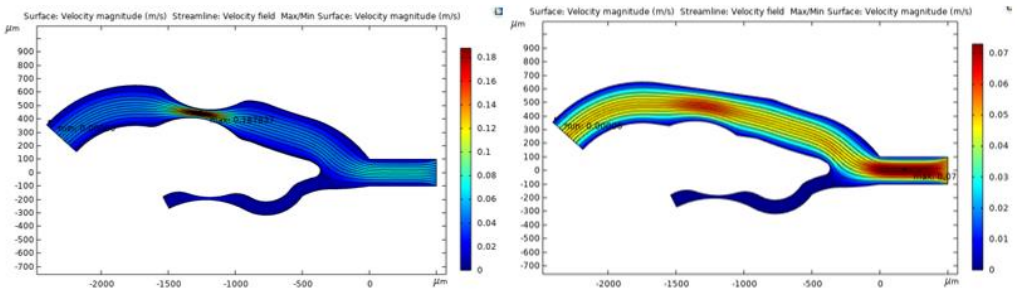

Figure 4.6 Vascular constrictions which have 70 µm (Left) and 220 µm (Right) section diameter

In other two analyzes, flow simulation was evaluated on different vascular constrictions which have 70 µm and 220 µm length. The velocity profile diagrams are shown below. The maximum point of the change in velocity due to the narrowing of the vessel is in the contraction modeling, which is 70 µm wide. The maximum velocity was measured as 0.187 m/s in the middle of the contraction. In the vein narrowed to 220 micrometers, the maximum velocity is seen in the main channel, not in the narrowing. This is because the radius of the main channel is greater than the contraction.

4.2 Liver-on-a-Chip Design

The following Liver-on-a-Chip design were formed step by step. First, the channel where the nanoparticle will be included in the system was connected to the normal flow system through a separate channel. Then, the mixing part was drawn. Finally, the microfluidic chip design was obtained.

4.2.1 Nanoparticle introducing on chip modeling

The microfluidic chip design below has two inputs which have 100 µm diameter; one of them was introduced for fluid flow and the other one was for nanoparticle introducing. Both inputs got together at the end of the 400 µm length of the nanoparticle channel.

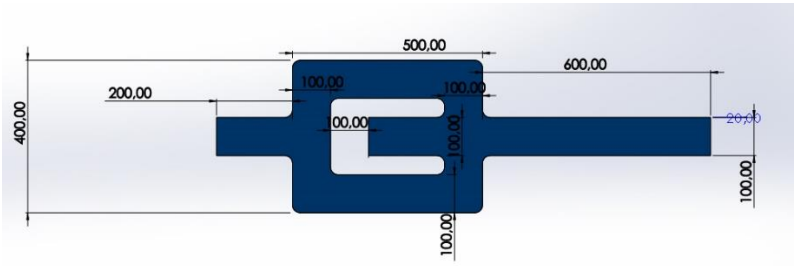

Figure 4.7 Technical Drawing Nanoparticle Introducing on Chip

Technical Drawing was imported as .dxf file which was obtained from SolidWorks to COMSOL Mulphysics program by using “Geometry” window. The domain was selected µm because of the all measures on drawing is on microscale. The material selection was made as water due to the ease of observation.

From “Physics” window “Laminar Flow” and “Transport Diluted Species” were added to work them together at the end of the present analysis. In laminar flow section flow properties (density and viscosity) were transfered from material. Then it was informed to the inlet of the design. Initial driven force was chosen as pressure and initial pressure value is 20 Pa. Then, from “Transport Properties” tools the diffusion coefficient was selected as user defined and isotropic 10^{-2} m^2/s. The transportation species were introduced from the inlet where the channel is inside of the loop.

The study was performed “Time Dependent” in time interval 0.1 - 1 s for both physics type. The results were shown on figure 4.9 with respect to time. At the beginning of the simulation the comcentration has the maximum value on just near the line where was the species transferred. The arrows show the concentration dissemination on the microfluidic chip. They are weak at 0.1s of the simulation however they have gained strength when the simulation reached 1s. The concentration spread around all over the chip at the end. Values were taken from specific points along the channel. While the values are 0.24, 0.16, 0.10, 0.27 mol/m^3 respectively on the road of the chanel at t=0.1s, at t=1s, end of the simulation, the values are approximately 0,67 mol/ m^3 through whole the road. It appears that the concentration flux stabilizes as time passes.

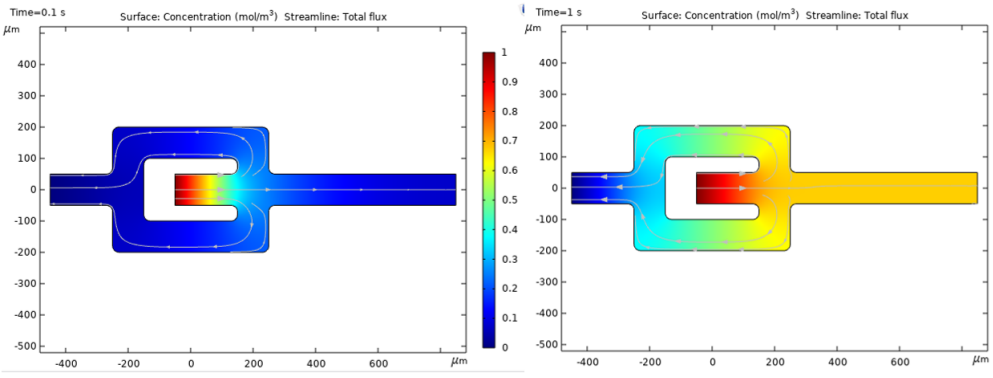

Figure 4.8 Concentration Flux of Transport Species on Nanoparticle Introducing on Chip t=0.1s (left), t=1s (right)

At the same time, velocity and pressure graphs were obtained. It is shown on the figure 4.9 that while the velocity values have maximum $0{,}35x10^{-2}$ m/s as an initial value, maximum velocity magnitude approaches 10 times the initial value at t=1s. From the

another point of view, the velocity obtained from inlet equally divides into two geometrical equal seperate channels. Then, when the channels join after 400 µm loop channel, the velocity doubles again.

When looking at the pressure contour, the pressure values are decreasing order starting from inlet towards outlet. The lattering of the pressure seems more linear at t=0s, while they take wavy shape at t=1s and is able to reach of the pressure 20 Pa.

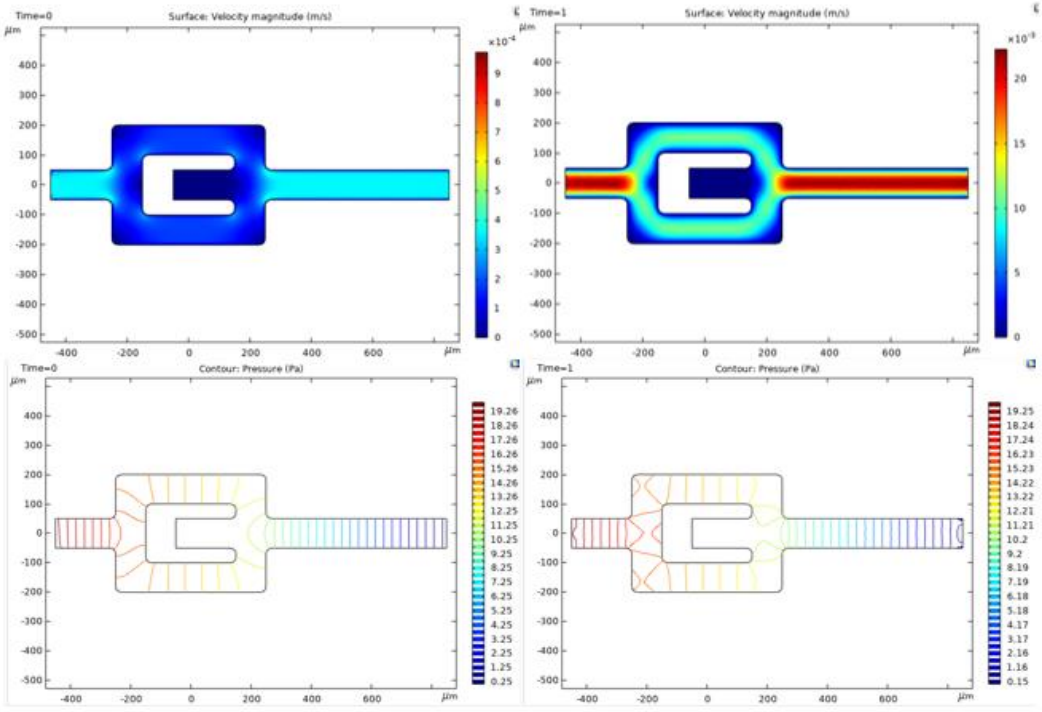

Figure 4.9 Velocity Profile and Pressure Contour Graphs on Nanoparticle Introducing on Chip

4.2.2 Nanoparticle & fluid mixing on chip

For the second step the nanoparticle and fluid mixing was achieved by creating gradient driven transport. The design was done by using eight geometric mixing structures. Those structures has 50 µm diameter protrusions, from the 30° far away the main channel. There is 150 µm distance between two protrusions.

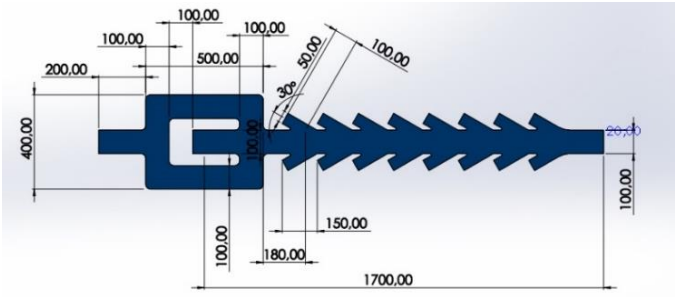

Figure 4.10 Technical Drawing of Nanoparticle and Fluid Mixing on Chip

The CAD drawing was imported to COMSOL Multiphysics. In geometry toolbar the unit was set µm and selected drawing was built. Then in the model builder window, material selection was done as water. The computational domain in which the micro flow of the selected material in the geometry added of the simulation program should be performed was determined.

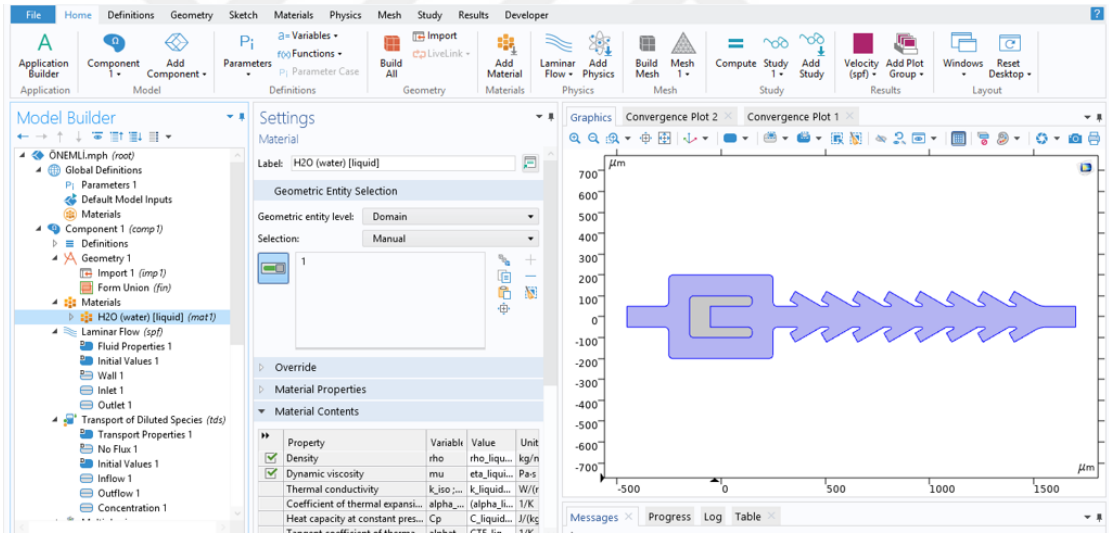

Figure 4.11 Domain Selection

In the present section of the study, two different "Physics" was combined: "Laminar Flow" and "Transport Diluted Species". In "Model Builder" window Laminar Flow was chosen. Inlet and outflow of the fluid was added and the rest of boundaries were set as wall. The flow was set as Pressure driven (P_0= 20 Pa).

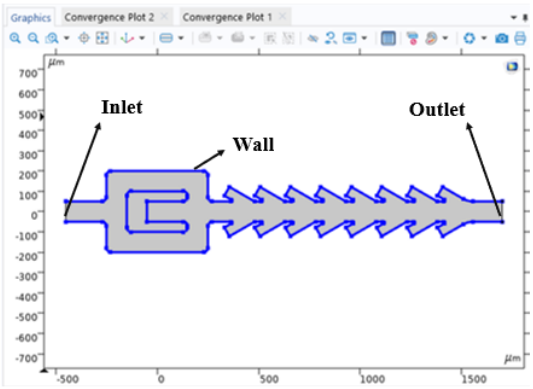

Figure 4.12 Inlet, Outlet, Wall Determination

In order to obtain a mixture at the end, diluted species was introduced from the microchannels by using "Transport Diluted Species" Physics window. The middle channel of the microfluidic device was considered boundary in laminar flow, but this time adjusted to provide a certain concentration of fluid flow as shown on figure 4.13. From "Transport Properties" toolbar velocity field was chosen "Velocity field (spf)" which comes from the Laminar Flow section. After that "Water" was again added as material, "Diffusion coefficient" was adjusted "User defined" as 10^{-2} m^2/s.

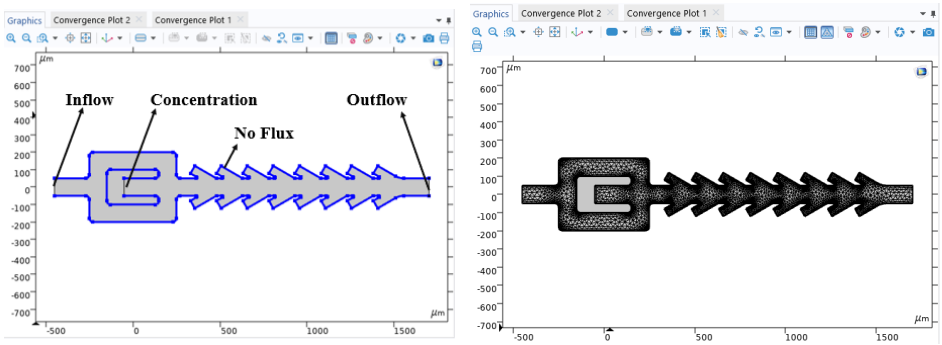

Figure 4.13 Inflow, Outflow, Concentration and No Flux Determination (left), Physics Controlled Mesh (right)

Inflow and outflow concentration has zero value, while source selection was adjusted as 1 mol/m^3. From the right click of "Multiphysics" window "Reacting Flow, Diluted Specieis" was selected. "Coupled Interfaces" was checked. Afterwards, "Physics Controlled Mesh" was built on chip. From the "Study" window "Time dependent" was added to observe the flow and concentration simulation based on time. Finally, the study was computed.

Data which were obtained from simulation were catagorized and analyzed into 3 sections: Velocity, Pressure, and Concentration.

4.2.2.1 Velocity analysis

The velocity profile of the microfluidic device shows that the maximum velocity is 0,016 m/s on the midpoint of the main channel and minimum velocity is 0 m/s on boundaries. While the main channel divded into two subchannel the velocity was also divided into two (appx 0,008 m/s). The arrows which show the magnitude and direction of the velocity were getting weak while the velocity were decreasing and vice versa. On the mixing structures' wings, the profile changes suddenly from 0,016 m/s to 0,012 m/s. The changes were repeated eight times through the eight mixing structures.

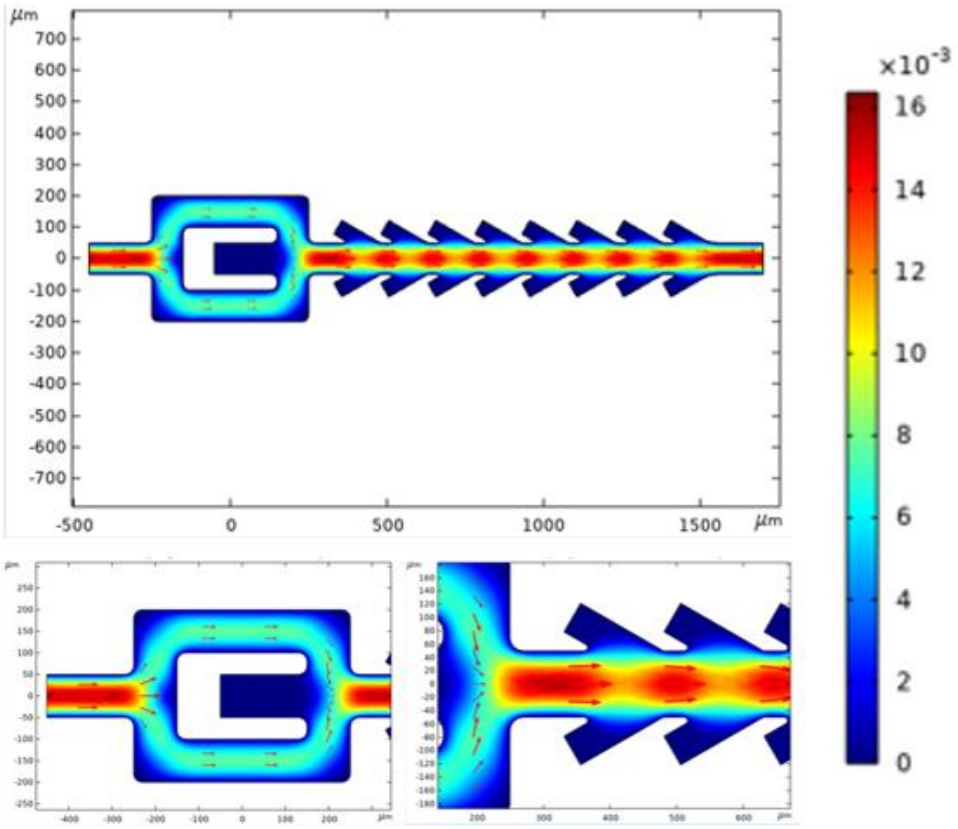

Figure 4.14 Velocity Profile of Nanoparticle and Fluid Mixing on Chip when t=10s

4.2.2.2 Pressure analysis

Pressure contour shows that 20 Pa which was introduced from the inlet of the microfluidic chip decrease to 0.24 Pa. Velocity changes affected the pressure values.

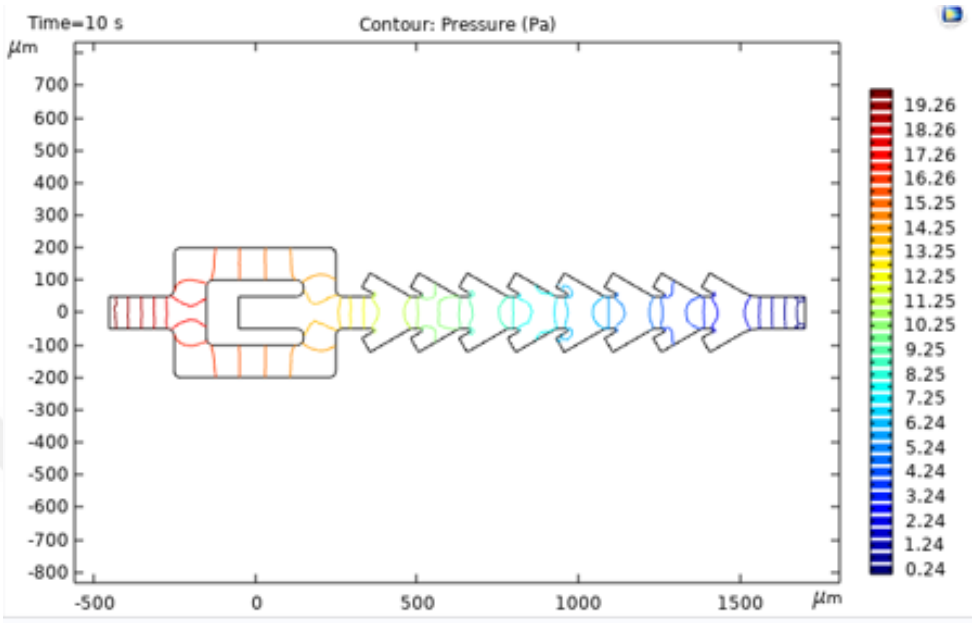

Figure 4.15 Pressure Contour Grapf of Nanoparticle and Fluid Mixing on Chip when t=10s

4.2.2.3 Concentration analysis

Transporting diluted species analysis were observed on Concentration Flux data. There were two sections that taken at 10th and 50th seconds. According to the color scale representing the density of the concentration, there are differences between ten seconds to fifty seconds. Color getting darken over time. Also, the arrows which shows the concentration getting stronger and linear to the end of the channel. Maximum Concentration value is 1 mol/m^3 on the channel input where the transportation was introduced and the minimum concentration flux is recorded approximately 0,65 mol/m^3.

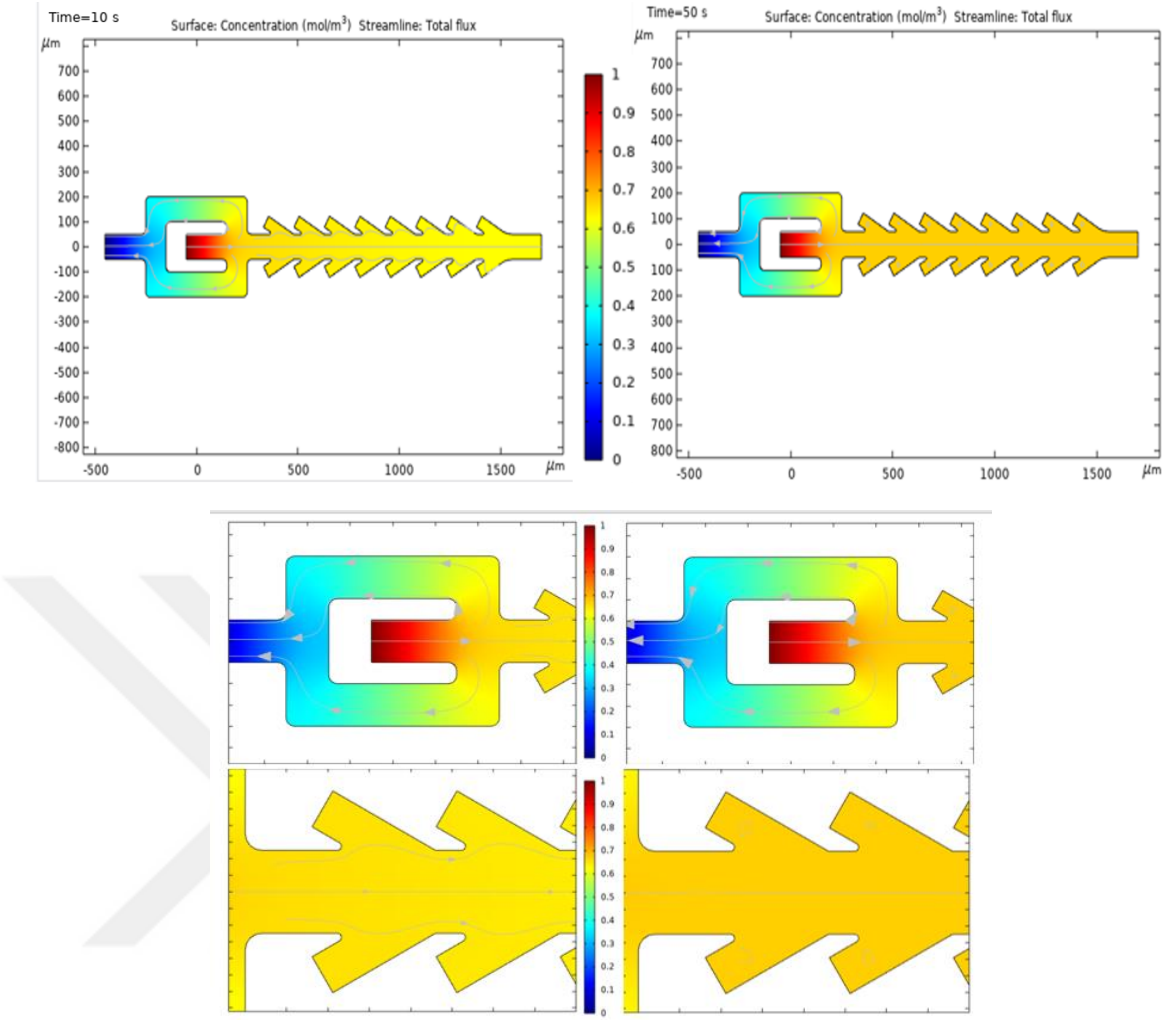

Figure 4.16 Velocity profile with respect to time

When looking deep it was realized that the concentration increased in the loop from the conctration intrdoduced part to the flow inlet part. Furthermore, at 10th second concentration arrows have weavy shape through the mixing structure. However they got directional shape at 50th second through the structure. Also, on the wings the arrows take circular shape.

4.2.3 Liver-on-a-Chip

The final design was drawn by adding actual microfluidic chip part. The chip was formed 100 mm length and 800 µm width rectangular shape and has sixteen microwells which

each of them has 100 μm diameter. The fluid and nanoparticle mixture was sent through four channels from main channel. At the end, the all fluid was collected through four output channels to main end channel.

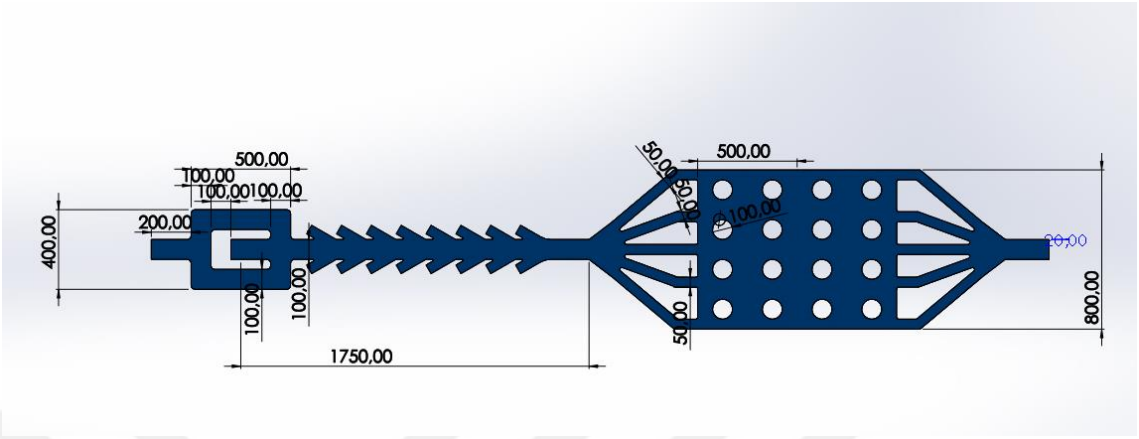

Figure 4.17 Technical Drawing of Liver-on-a-Chip

Analysis was initiated for the entire chip in line with the data obtained from previous liver-on-a-chip fragments.All the parameters which are taken from the physics, materials, mesh, and study window are same an valid for liver-on-a-chip system. Apart from previous studies, two different observations were obtained by giving 20 Pa pressure value and 0,5 m/s separately as initial force in liver-on-a-chip design. Transporting special diffusion coefficient was set again 10^{-2} m^2/s. Laminar flow was introduced from the inlet of the chip and transporting species was from the inlet of the loop. Time dependent study was worked for those two types of physics in time interval 0.1s to 1s.

4.2.3.1 Velocity analysis

The analysis were evaluated on velocity magnitude graph shown on figure 4.19. The “a” plots show the velocity (v = 0.5 m/s) driven simulation, when the “b” plots show pressure (P = 20 Pa) driven simulation. It was shown that when time = 0, a1 has 0.3 m/s maximum velocity magnitude, it is reached 0.5 m/s when t = 1 s (a2). In the liver-on-a-chip system, the velocity equivalent of 20 Pa corresponds to 0.04 m/s at t=0 s (b1), while it corresponds to a speed of 0.06 m/s at the end of the simulation (b2). On the boundaries no slip condition works, it means that the velocity is 0 m/s on boundaries. However on “a3” plot (left), near the boundaries show some velocity profile, while “b3” show more boundary.

At the same time, on mixing structures it is shown that the wings on “b3” (right) have more color scale when compared to a3 (right). Moreover when looking at the a4 and b4 plots, it is evaluated that the fluid flow were divided into 4 subchannel. In consewuence of that the velocity magnitudes are also divided into four. But it is realized that the middle three channels have a faster flow than the channels at the sides on a4 plot. The difference is approximately 0.3 m/s. But, on b4 plot the velocity difference (almost 0.005 /s) between the middle channels and side channels is not huge.

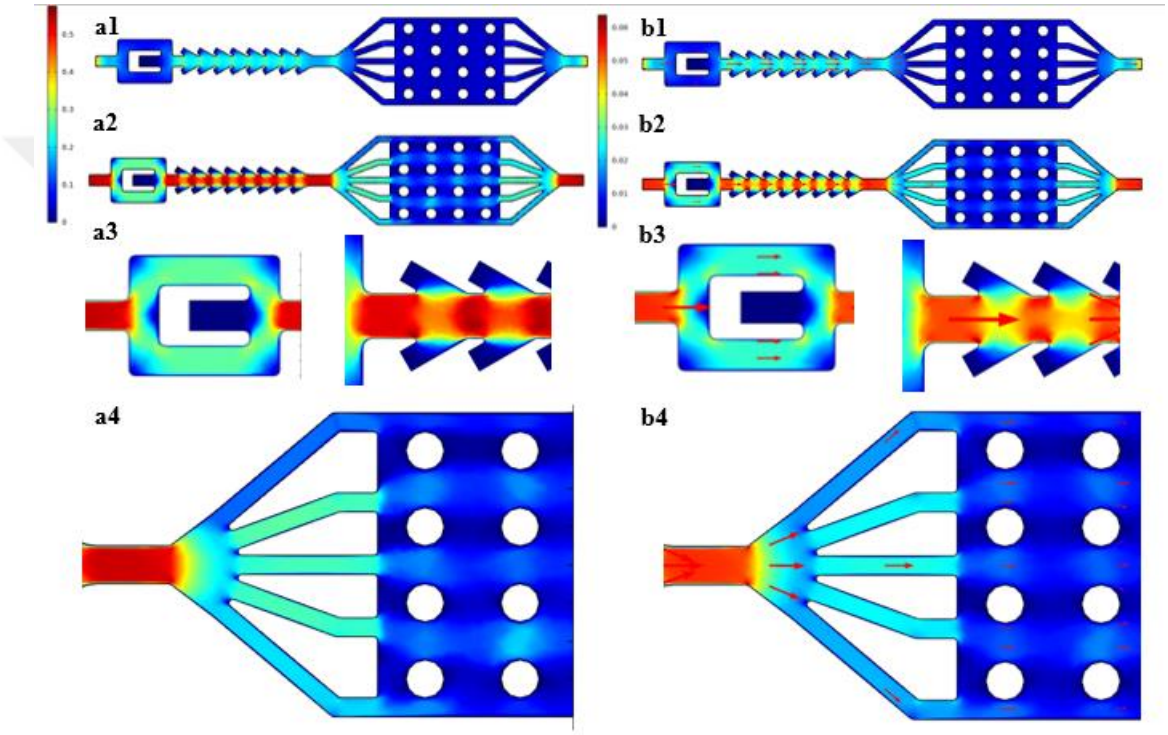

Figure 4.18 a=Velocity driven simulation (1:t=0, 2: t=1s, 3 t=1s, 4: t=1s); b= Pressure driven simulation (1:t=0, 2: t=1s, 3 t=1s, 4: t=1s) on Liver-on-a-Chip Design

4.3 Tumor-on-a-Chip

4.3.1 Tumor spheroid modeling

In the present section the tumor spheroid design was aimed by taking inspiration form hanging drop method. The 2D technical drawing has a base and a semicircle which hanging over it. Base is formed 400 μm length and 200 μm width and the circle has 200

µm diameter. The contact line of the base and circle was changed from 100 to 200 µm at 50 µm intervals

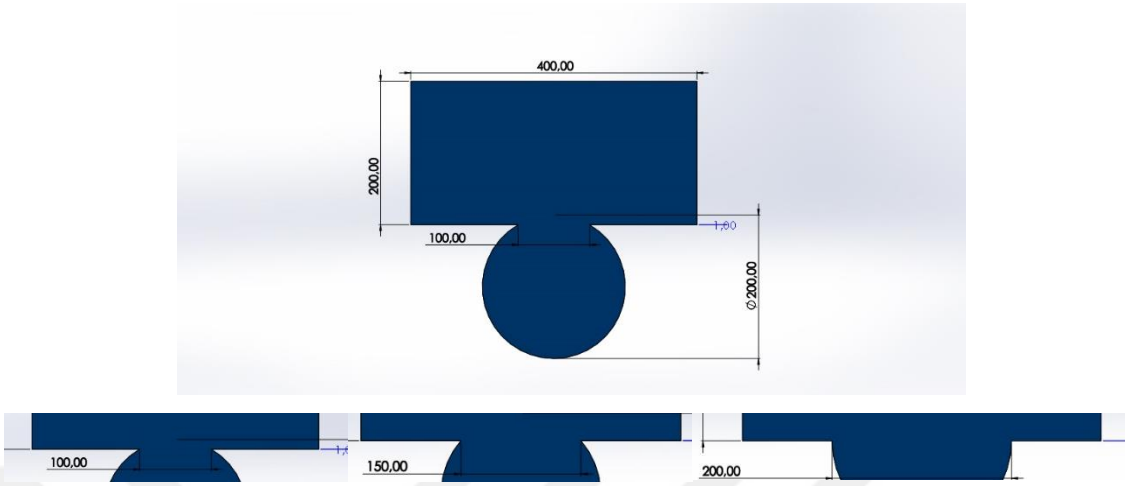

Figure 4.19 Tumor Spheroid Modeling 100, 150, 200 µm contact line from right to left

When the technical drawing was completed it was imported to COMSOL Multiphysics geometry platform in microscale and 10^{-5} tolerance. Then, the material which flows on microfluidic device was added. For tumor spheroid microfluidic designs RPMI that is acronym of the "Roswell Park Memorial Institute" as a kind of culture media was chosen for fluid flow. In the widespread use of RPMI, 5% FBS (Fetal Bovine Serum) is added to its content. In present study the mixture of DMEM and FBS was used. In order to define material properties density and dynamic viscosity of mixture were identified as 1002 kg/m^3 and 0.848 x 10^{-3} kg/m.s respectively (Poon, 2020).

Laminar flow physics was selected for observation the contact line of tumor spheroids which were designed beginning from 100 µm to 200 µm length and the regarding changed angle. Inlet and Outlet of tumor spheroids on chip were shown on the figure 4.21. From the inlet part of the device inflow velocity was adjusted 0.05 m/s.

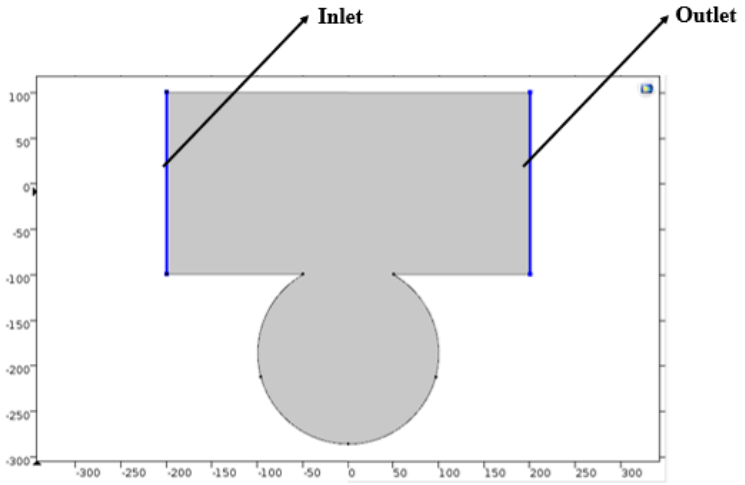

Figure 4.20 Tumor Spheroid Inlet & Outlet Part

Physics controlled mesh and stationary study were applied. The results were evaluated for every design below. The point to focus on is the velocity profile on the semicircular recess hanging on the simulation. It is clearly seen on the simulation that while the contact line of the base and circle increase the streamlines of velocity get wavy and they get close the boundaries of circle. On the other hand, the velocity profile on the way of the microfluidic design is nearly same both three hanging drop tumor spheroids.

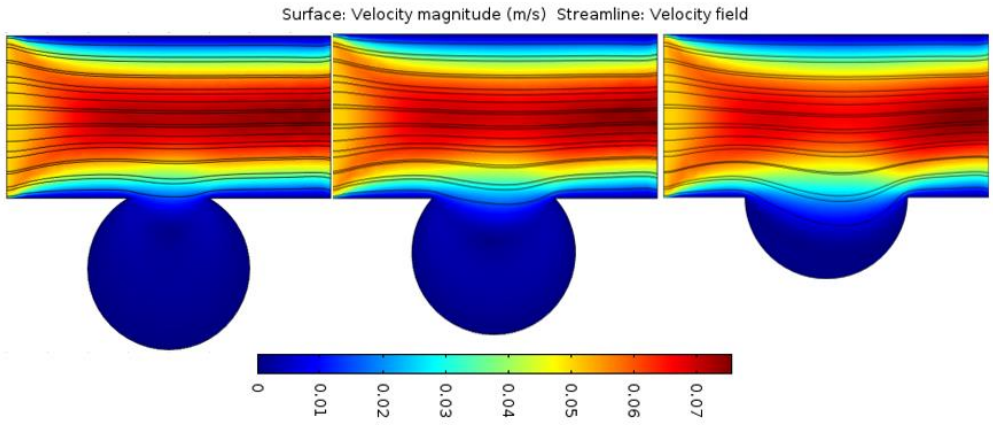

Figure 4.21 Tumor Sphereoid Models Fluid Flow Simulation

4.3.2 Nanoparticle introducing on Tumor-on-a-Chip device

In the present tumor-on-a-chip modeling spherical tumor was designed in SolidWorks software program. It consists of three main channels that have 100 µm length. The outer

channels are specified for endothelial cells flow vascularization while the inner channel show the tumor vasculature. The big circle in the middle has 850 µm diameter that is for mimic tumor structure. The little channels between the big circle and the outer channels show "enhanced permeability and retention effects (ERP)" gaps. They have 50 µm diameter and 100 µm length. The angle between little channels was adjusted as 35°. The whole length of the microfluidic device is 2500 µm.

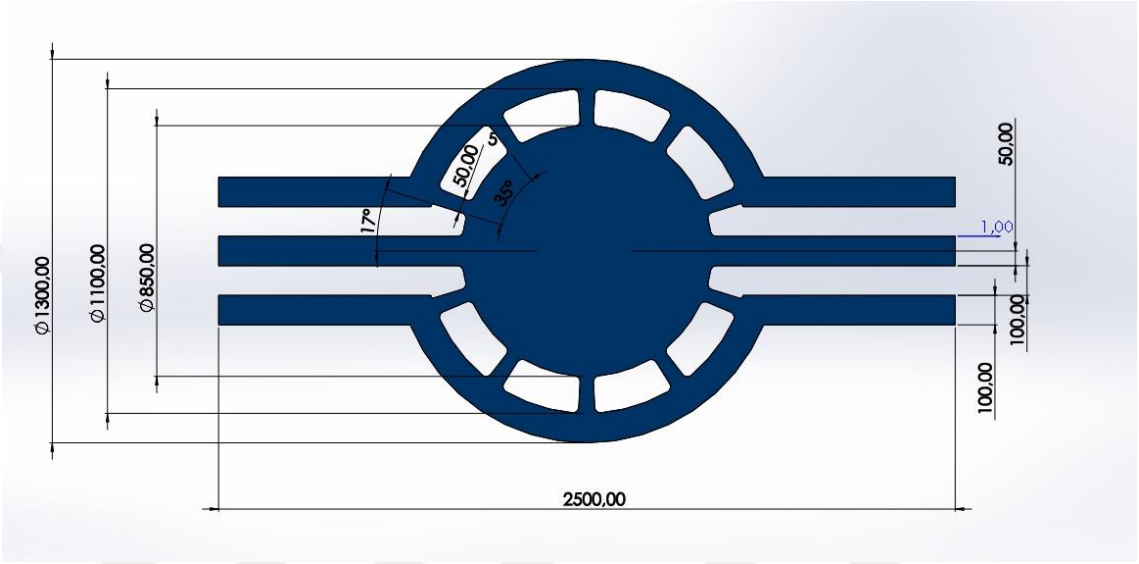

Figure 4.22 Tumor-on-a-chip design

After 2D schematic design of the tumor-on-a-chip, the dxf format of the draw was imported to the COMSOL Multiphysics. Then, since "DMEM + 5% FBS" mixture material is not available in material library it was added manually. Density and dynamic viscosity information from material contents was selected in order to enter values. DMEM + 5% FBS density was introduced 1002 kg/m^3 and it's dynamic viscosity was introduced as 0.000862 Pa.s. The domain to allow the flow of liquid was defined.

After that, two different physics (Laminar Flow, Particle Tracing for Fluid Flow) was added from Setting window. In laminar flow section, density and the dynamic viscosity of the fluid flow was adjusted as taken from material. The walls, input and output were defined. No slip boundary condition was accepted fort he walls of the chip. The initial velocity of the fluid was entered 0.05 m/s.

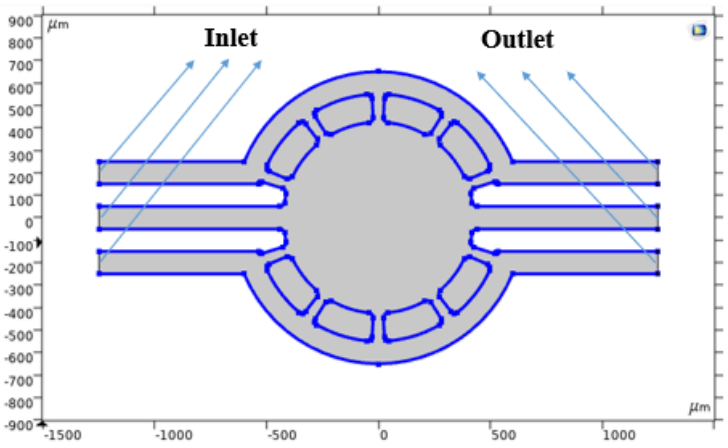

Figure 4.23 Inlet and Outlet Channel of Tumor-on-a-chip Model

In particle tracing for fluid flow physics, "Wall condition" was selected "bounce". From "Particle Property Specification" window, particle density and diameter was introduced 2267 kg/m^3 and 100 nm respectively. The 0 charge number was written. Channels surrounding the chip were selected for the inlet through which particles enter the microfluidic chip. The particle relase time was adjusted by chosing "Distribution Function" then clicking "List of values" and adjusting range(0,1,1). In order to determine initial position of the particle 100 pieces was written on "Number of Particles per Release". The initial velocity was selected from "velocity field (spf)". From forces window Gravity and Drag Force was added. The gravitational force to act on the particles was added in the y direction as -g m/s^2. Drag force was set to affect the particles as "velocity field (spf)".

"Mesh Settings" was selected as physics controlled extremely coarse for both Laminar Flow and Particle Tracing for Fluid Flow physics. Two different studies were initiated due to the application of two different physics on the design: Stationary and Time Dependent. Laminar flow was run in stationary while the particle tracing for fluid flow was analyzed in time dependent study. In time dependent study initial values of variables solved for "Physics Controlled".

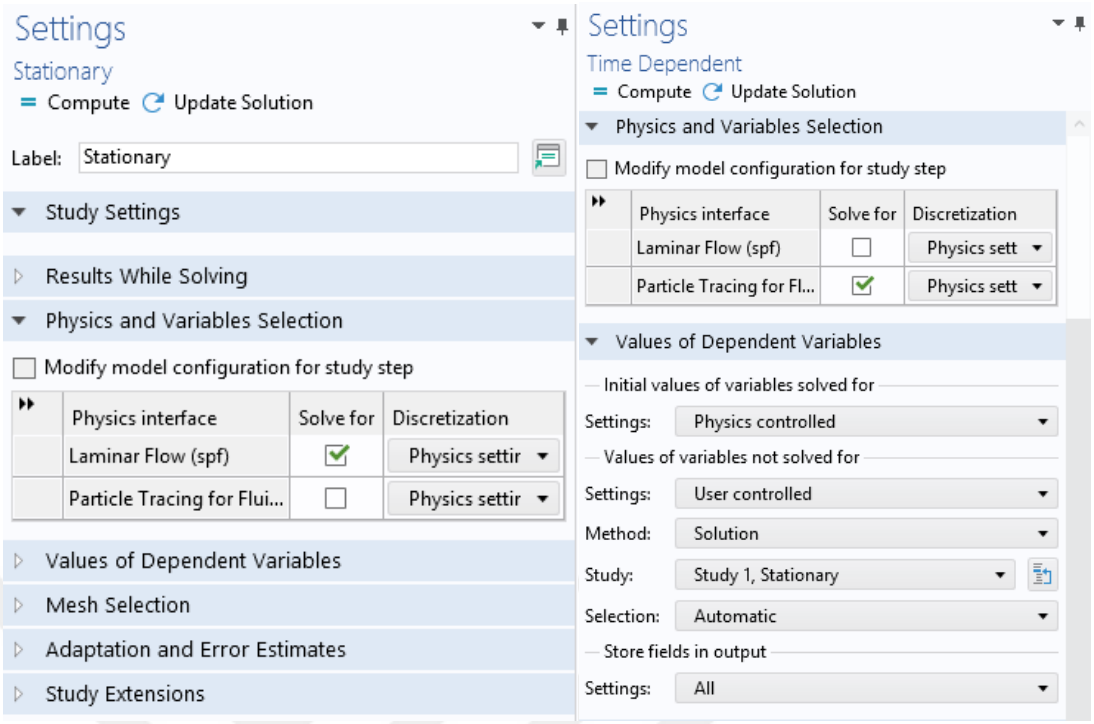

Figure 4.24 Study Settings

The velocity analysis of the tumor-on-a-chip device was done and shown in the figure 4.6. While the inlet channels have the same velocity profile outlets have different profiles between each other. The maximum velocity approximately 0.08 m/s is on the midchannel. DMEM + 5% FBS fluid flow was observed also through small channels. Those subchannels strengthened the fluid flow inside of the tumor-on-a-chip. While the velocity increased outlet channels, pressure increased through the microfluidic device. The pressure value was calculated 95 Pa at the beginning and 2 Pa at the end.

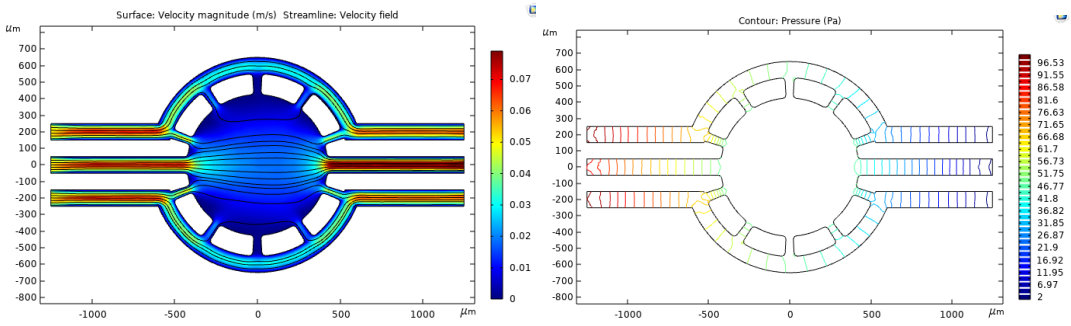

Figure 4.25 Velocity (left) and Pressure (right) Analysis of Tumor-on-a-chip

Time interval of the analyze was adjusted 0 to 2 s. At t= 0.1 s, the particles show velocity distribution in a pipe same as parabolic in shape. When 100 particles with a size of 100 nm sent during the liquid flow period are examined, all particles fellow the streamline of the velocity. No particle flow was observed from only one of the small channels on the microfluidic chip. At the same time, the particles are affected by the velocity while flowing through the chip, and there is a slowdown in their movement towards the middle of the chip in the direction of this velocity.

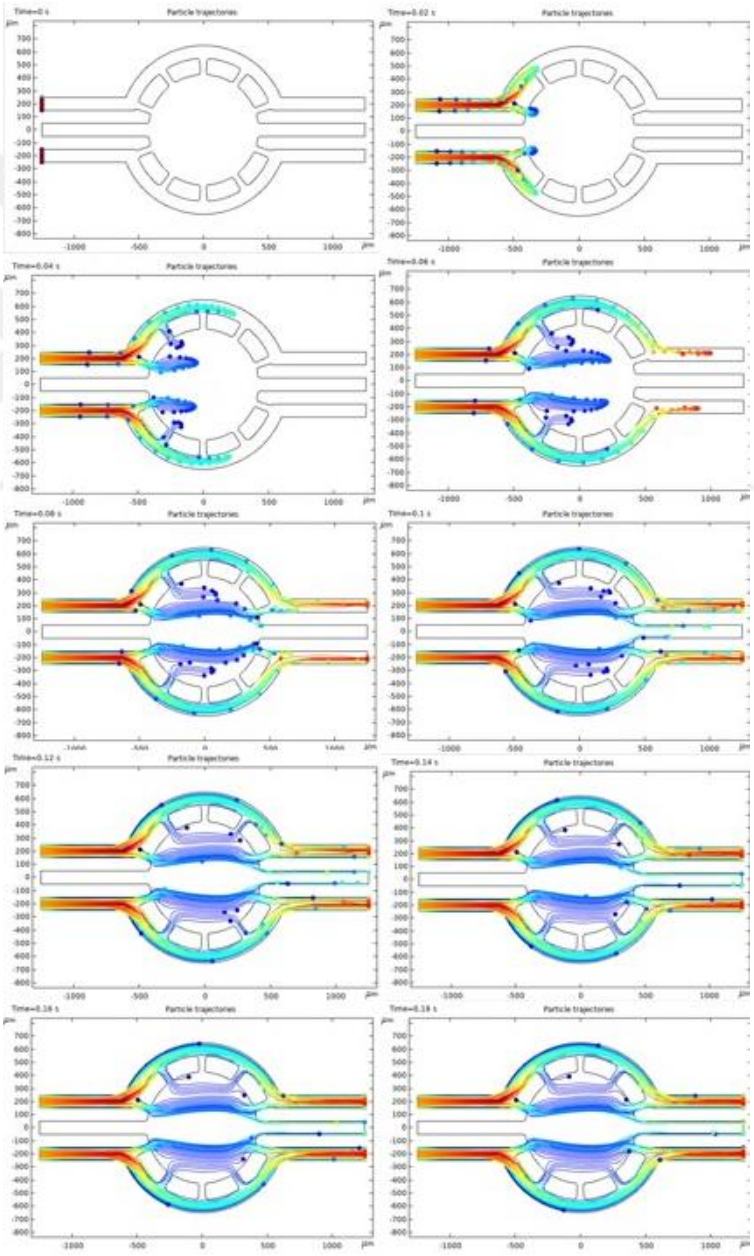

Figure 4.26 Nanoparticle Tracing on Tumor-on-a-chip (0 to 0,18 s)

5. DISCUSSION AND CONCLUSION

Microfluidic chips can be explained as *in vivo* like *in vitro* systems. The similarity comes from the possibility to create a microenvironment of the cells on microfluidic devices. Knowledge of the interactions between the cells and their microenvironment is significantly important. Furthermore, before the fabrication of organ-on-a-chip devices prediction of some parameters which are flow, shear stress, pressure, etc. can be considered as vital in order to decrease excessive usage of chemicals, cells, time.

In the present study, organ-on-a-chip systems were designed in SolidWorks and simulated in COMSOL software program. The aim of the following studies were to examine the predictable microfluidic behaviors and examine the behavior of the nanomaterial in a microfluidic system before performing an organ-on-a-chip design in real time. From this perspective, first, some basic fluidic behaviours were examined in "Branched Vessel Modeling".

The vascularization in humans is in a form that covers the whole body and has a reticulate structure. The diameter of the vessels from the aorta, which is the largest vessel, to the capillaries, and consequently the flow rate varies. The branching structure in the vein is the most commonly used type in microfluidic chips. Since the transportation of the culture medium used in cell culture and the delivery of the nanomaterial will be through these channels, the qualification of the channels (vascular structure) is important.

The fluid transferred from the main channel at a velocity of 0.1 m/s, then it decreases in velocity (approximately 0.55 m/s) at subchannels. Then, by dividing these two subchannels into two, the velocity again decreases (approximately 0.045 m/s). This situation can be explained with Bernoulli's flow contunity equation. Besides, in the middle of the channels it's shown that the velocity of the fluid is highest. This situation is expected because of the no-slip feature which induce the fluid flow near the wall approaches zero. The effects of the no-slip condition interactions cause decrease of the velocity on neigboring particles. At the end, the parabolic velocity profile was obtained

in laminar flow. The parabolic pathway means that your cells/culture medium or concentrated fluid which containes nanoparticles will follow on.

In order to compare sharp and shoft edges effects on microfluidic behaviour the simulation was run also for shoft edges. The parameters which are technical drawing, material, inlet and outlet, initial velocity, and mesh were kept same with sharp edged design. As shown on the figure 5.1. the shoft edges show lower velocity profile when compared to sharp edged microfluidic chip. It means that no slip boundary condition show it's own properties edges. Shear stress is also low on soft edges due to low velocity profile. Thus, since there will be less shear stress on the cells, microfluidic chip-based cell deaths will be prevented.

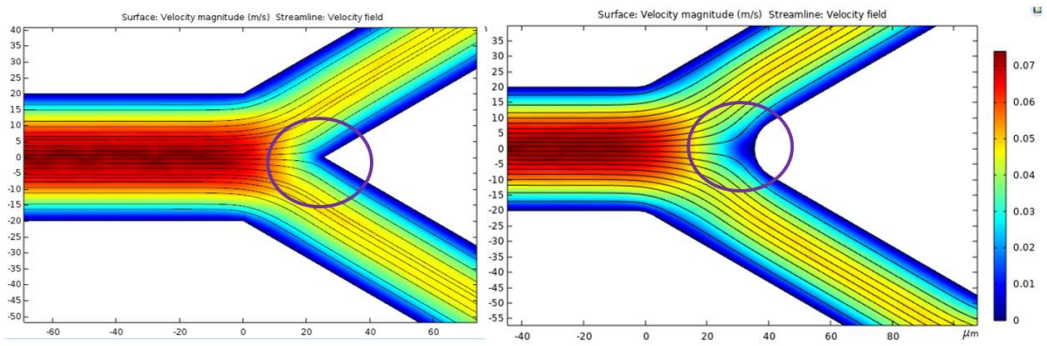

Figure 5.1 Velocity Profiles on Edges: Sharp (left), Soft (right)

As a final thought of the branched vessel modeling on chip, it can be said that there should be some considerations while designing: the diameters of the vessels should be adjusted by taking into account of the desired velocity obtained at the end of the chip. It means that reverse engineering should be performed. Moreover, the sharp edges always cause high velocity and accordingly cell death when fluid flows. More oval, soft edges can be more appropriate for sensitive cellular behaviour. Finally, due to laminar flow properties, the cells can be easily observed on the streams on microfluidic chips. The imaging techniques of cellular issues can be adjusted by considering those features.

For cardiovascular and cerebrovascular diseases blood vessels have significant importance. A possible cause of cardiovascular diseases is vascular occlusion which is

formed of deposition of fat or cholestreol plaqueon the blood vessel walls. Furthermore, the forming of deposition may cause cardiac arrests or heart attacks. In clinics, early diagnose of those kind of diseases or analyzing occlusions is essential (Shakya & Chowdhury, 2019).

Different types of vessel obstructions model were evaluated in "Microvascular Occlusion on Chip" study. When paid attention on the designs which same obstruction length but formed in different way, the maximum velocity is same. However, the increased velocity pattern in velocity profile analyze, it was clearly shown that the pattern has wider area on single obstructed vessel modeling than double formed one. This situation has an vital importance consequence: sudden changes on vessel walls cause sudden changes in velocity. In other words, if the occlusion is formed slowly in gemoetrically, the velocity increase results slowly and revert it's normal velocity slowly. But in geometrically sharp changes cause sharp increase ann then decrease suddenly. A sudden blockage can also occur when a clot breaks off (turns into an embolus) from an area such as the heart or aorta, passes through the bloodstream, and is located in a downstream artery. Consequently, double sized obstructed vessel diseases should be considered in deatil because they may have high risks for patient's life.

Addition to the sudden blockage vital cansequences, there are also some problems with possible nanomaterial/drug treatments for vascular constriction. When the velocity of the fluid increase in these regions which are narrowed, drag force of normal circulating plateles increase due to high shear stress in microfluidic device. It causes rapidly adhering of those platelets to the wall of the vessel which is known as major factor of forming plaques. Ischemic stroke, pulmonary embolism or coronary infraction which occur due to obstructed vessel require acute emergency action. In the double-sided vascular occlusion model, 50 nanoparticles of 1 nm size were identified and sent from the input. While the nanoparticles move on the laminar flow streamlines until they reach the occlusion zone, they cannot continue their movement on the same streamline after the occlusion. They continued their movement on streamlines in an area of occlusion width which is 166 μm.

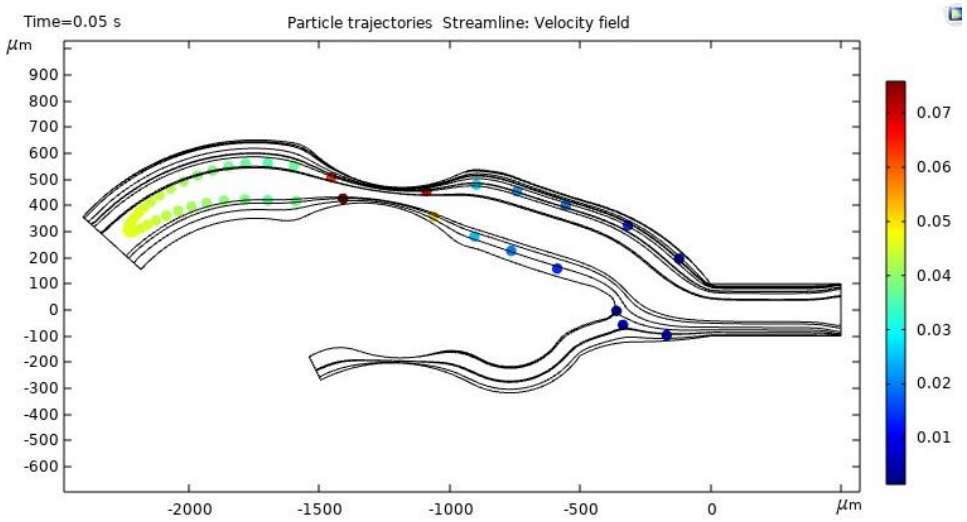

Figure 5.2 Double-sided vacsular occlusion particle tracing simulation

There is a physics behind this obstruction-nanoparticle mechanism: Drag Force effect. Drag force is called fluid resistance that cause opposite force to the relative motion (Kolev, 2005). For example, when driving on the highway in a car, you have to split the air, which is a fluid. therefore, a force proportional to the square of your velocity counteracts your movement. The same applies to submarines, fish, etc. that move in water. This force increases if you go faster, increase the cross-sectional area (as in the parachute), or move in a denser fluid. The magnitude of the force depends on these parameters, but it also depends on the shape of the object. The formula of the drag force can be summed as:

$$F_D = C_D A \rho \frac{\nu^2}{2}$$

Where;

F_D = Drag Force

C_D = Drag coefficient

A = Area

ρ = Density of Fluid

ν = Velocity

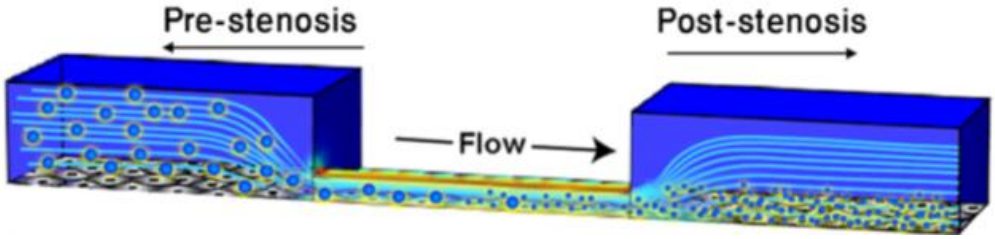

Figure 5.3 SA-NTs motion on microfluidic vessel obstructed model (Korin et al., 2012)

In order to receive effective and immediate treatment to the vessel plaques, nanomaterial based solution can be offered by taking advtange of drag force. In 2012, Netanel Korin *et al,* developed shear-activated nanotherapeutics (SA-NTs) which are at microascale size but fabricated of multiple nanoparticles (NPs). These are liken plateles but when they exposed high local shear stress they are broken up in nanoparticle form. In this manner, those SA-NTs can be concentrated on obstructed vessel wall and furthermore overcome possible cardiovascular diseases (Korin et al., 2012).

When the other "Microvascular Occlusion on Chip" designs are examined in detail, there should be focus on inlet velocity and maximum velocity at the middle of the blockage. While the inlet velocity is 0.05 m/s, the maximum velocity was recorded as 0.187 m/s. There is a huge difference between those velocities when considered microscale platform. It can be explained with Bernouilli's equation. According to the formula of Bernouilli's equation the velocity is changed exponentially, that is, the square of the radius. It means that, little obstruction vessels may cause serious helathy problems.

In other part of the present study, the liver-on-a-chip design was evaluated into three subsection: Nanoparticle Introducing on Chip, Nanoparticle & Fluid Mixing Structure and total Liver-on-a-Chip System. In the first section it was aimed that how to transport diluted species into a microchannel. Decision of the road that the diluted species transfer was so important. If the dilution sent to a side of the channel, the dilution dispersion tendency would not be uniform. In order to overcome this nonuniform motion, inlet and inflow line was designed horizontally on same position. Also, the laminar flow first divided into two subchannel. When the subchannel met again, the diluted species got in those two channels to form a uniform flow.

The concentration gradient arrows goes both to outlet and inlet of the microchannel. 1 mol/m^3 initial particle concentration decreases while the flow gets further because of the Fick's Law of Diffusion. In real microfluidic chip design the distance and decrease in Concentration should be considered. If it ignores, significant data may not be obtained since the rates of exposure of cells located close and far away on the organ-on-a-chip to the drug or nanoparticle sent at a certain concentration will vary.

The mixing of the Concentration gradient and the fluid is not clear in Nanoparticle Introducing on Chip design. Because of that, the second part of the section was thought. Mixing of the fluid and diluted species was aimed by designing a mixing structure.

There are several effective mixing strategies that increase the entropy. Mixing is a kind of process which use concentration gradient as a driven trasnport. Mixing can be applied by convection, turbulent diffusion, advection etc. However, while the diversity of mixing process are easy to achieve in macroscale, in microscale it is limited. Obtaining turubulent flow is difficult because of the dominant viscosity of the microscale units. Thıs, the efficient mixing method should be applied on microfluidic chips. Otherwise the streams of laminar flow become dominant and the concentration species follow the streamlines. If cells are introduced to the system since the cells will not be affected equally by the particles, it will be difficult to get the correct result. In this scope a mixing strategy was developed. The protrusions (wings) on the technical drawing are designed to allow the flow to enter these points and to mix the fluids at the outlet.

Table 5.1 Time vs Concentration on Liver-on-a-Chip Systems

Point	**@time=10s**	**@time=50s**
1	0.662 mol/m^3	0.674 mol/m^3
2	0.653 mol/m^3	0.672 mol/m^3
3	0.646 mol/m^3	0.672 mol/m^3
4	0.640 mol/m^3	0.672 mol/m^3

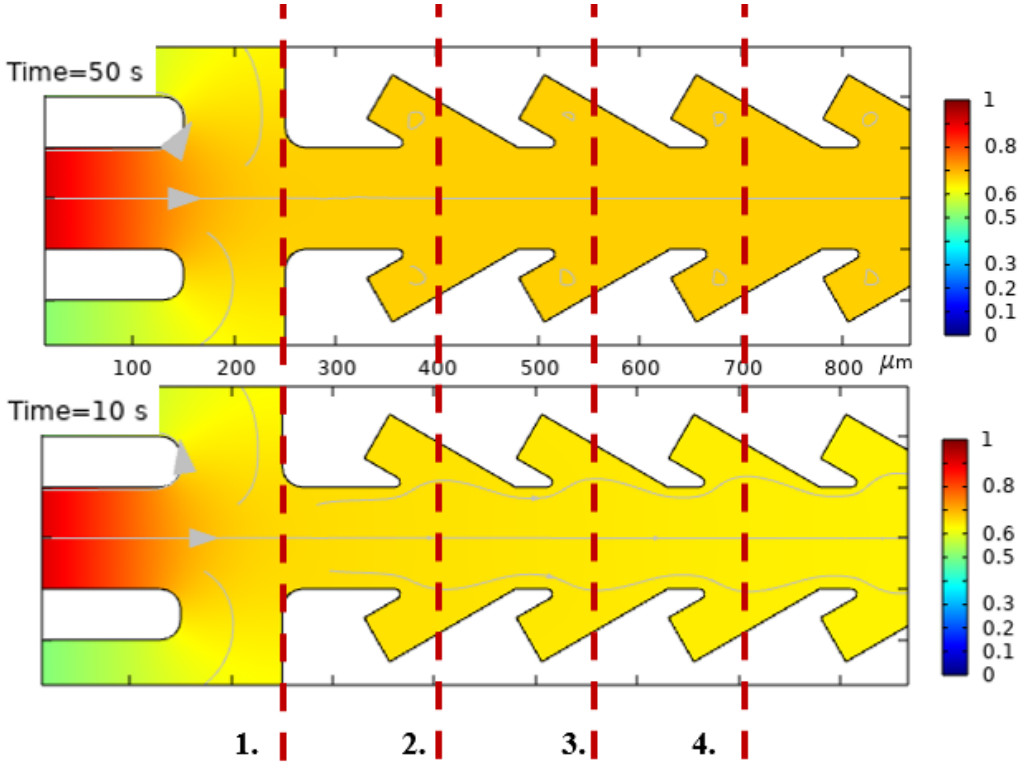

Figure 5.4 Streamlines of Concentration at t=50s and t=10s

While time passes, the concentration lines get stabilize. For better understanding four significant points were determined and the concentration data was recorded on table 1. Morover, it was understood from the arrows on microfluidic chip, the portrusions provide the reach mixing on transported species. The mixing strategy provide in real microfluidic chip to transfer homogenized species to the cells live in chip.

Last part of the liver-on-a-chip system consists of whole microfluidic device which is capable flow of cell and transport species at the same time and mix them. The important point of the liver-on-a-chip design is it's subchannels. If the fluid was sent to main chip by using single channel, fluid was flowed only the middle of the channel because of laminar flow properties. In the present study, the channels were divided four subchannels. Because of the division the laminar fluid flow characteristics was showed each channel inside. Furthermore, on the main microfluidic system the fluid is distributed every side.

Another point of the liver-on-a-chip system that should be considered is the wells on the chip. The wells is used for cell seeding. In the present study it was aimed to observe the

velocity profile near the boundary of the wells. While the fluid flow goes on near the wells, it was uderstood from the velocity arrows that near the wells boundaries the no slip boundary properties works. Wells are affected the velocity only on direction of the fluid flow. If the cells were seeded on those wells, their culture medium would refresh while the fluid flow continues.

For final inferences from liver-on-a-chip systems, there should be significant parameters. The driven force can be velocity or pressure depending on the generator of fluid flow. However, the velocity driven forces microfluidic systems seems easy to control due to complex width/diameter of chips. From another point of view of present study, the mixing strategies should be developed. Because in laminar flow the mixing operation manually may cause turbulent flow and so the shear stress can affect the cells inside the chip. Moreover, where the nanoparticle/drug transfere to the microfluidic chip is also significant decision. If they introduced with the same channel of fluid flow the concentration behaviour couldn't be controlled.

Tumor spheroid on a chip design was simulated to observe contact line effects on traditional hanging drop method due to the fact that it is a widely used method in the *in vitro* environment. However, in this case, the surface properties of the material on which the tumor spheroid will be studied come into play. The plate which the technique is applied on may have different hydrophilicity which affects radius and curvature of the drop. For example, on PDMS based plates and polystyrene based plates show different angles. When θ angle of the drop on PDMS is 99° the angle is 70° on Polystyrene biomaterial (Kuo et al., 2017). From other perpective of hanging drop tumor sphereoid method, it is known that control of contact line is difficult on same microfluidic chip material. However, Bin Gao et al, demonstrates that same volume could show different radius curvature by controlling spreading area. In hanging drop method the survival and formation of spheroids are significantly depending on the geometry and density of the cells (Gao, Jing, Ng, Pingguan-Murphy, & Yang, 2019). In the present study, the tumor spheroid was designed by using hanging drop geometry that have different conact line.
The purpose in doing this was to prove what effects surface forces can have on the designed work. The velocity streamlines show deep wavies on high contact line (200 μm)

design. It may provide high transmission of fresh culture media or drug to the cells on tumor cells which forms spheroids.

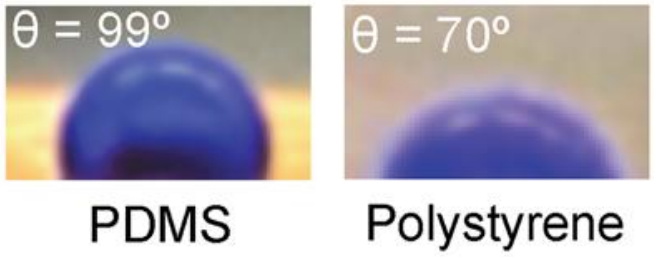

Figure 5.5 PDMS and Polystyrene hydrophobicity (Kuo et al., 2017)

In the present tumor spheroids-on-a-chip laminar flow simulation RPMI was used as culture media by mixing 5% FBS. RPMI is a kind of protein free culture medium. Selection of appropriate cell culture media is significantly important for microfluidic simulation for better mimicking of cellular microenvironment. They depend on the growth requirements of different cell lines. FBS is used for the attachment and proliferation of cells and it is a rich protein solution whose content is not fully defined. In this protein solution, hormones, enzymes, growth factors that enable its growth and reproduction. There are intercellular matrix proteins that allow it to be attached. Serum ratio in the medium according to cell type and applications can vary. In the present fluid flow simulation RPMI and 5% FBS was chosen for giving an example of modeling general usage of lymphoblast human cells.

Hanging drop designed tumor spheroid-on-a-chip models were evaluated into three different contact angles. Along with the contact line, the opening of the tumor mouth also varies inversely. The largest contact angle tumor spheroid formed (approximately 30 degrees) shows that it is very difficult for the laminar flow to penetrate into the tumor spheroid and reach the tumor center in this way. From other point of view, when the contact angle decreases and spheroid length increases, the laminar flow streamline begins to bend and wavy way into the tumor by staying away from linearity.

If it is desired to make some inferences at this point of the present simulation, the primary point to be considered in tumor spheroid-on-a-chip studies is the surface properties of the material. The materials most commonly in use on microfluidic chips are glass (or glass-derived), polystrene, and PDMS. When their hydrophobicities are sorted, they are known as polystyrene<glass<PDMS in bare form of the materials (Funano, Tanaka, & Tanaka, 2016; Kuo et al., 2017). If nanomaterials or drug materials would like to be studied, polystrene should be chosen in order to penetration inside of the tumor spheroids.

In addition to *in vitro* tumor spheroid-on-a-chip studies, the most common forms of tumor structures in real life have been the focus of organ-on-a-chip studies. Tumor structures have complex connections and irregular several blood vessels around themselves. Those blood vessels are tightly connect the endothelial cells. The connections between the tumor vasculature and endothelial cells have gaps which provides more nutrients to grow abnormally. They are called as “enhanced permeability and retention (EPR)” effect.

Vascular permeability in most tumors is higher due to the increased need for nutrients and oxygen. In normal vascular structures, molecules larger than 2 nm cannot pass between endothelial cells due to tight junctions. In the tumor region, as these tight junction areas are disrupted, macromolecules of 10-500 nm in size can pass into the tissue and accumulate in the tumor tissue. In addition, due to impaired lymphatic discharge in these regions, it becomes difficult for the accumulated molecules to exit the system.

Passive targeting is achieved by making use of these features of the vascular structure in the tumor area. This very remarkable feature is considered a milestone in tumor-targeted chemotherapy and is highly promising in anticancer drug development (Fang, Nakamura, & Maeda, 2011). In the present design, the EPR concept was aimed to observe nanoparticle/drug tranmission through them. The gaps between outer channels and tumor tissue provide nanoparticle or drug content passaging.

The aim of this part of the present study was to trace nanoparticles on the tumor-on-a-chip system to observe whether the nanoparticles would reach the center of the tumor by utilizing the EPR effect. When the results are examined, it is seen that microchannels are

very effective in inputs and outputs. Nanoparticles provide movement with the effect of gravity and drag force of the laminar flow which was obtained from steady state study and continue their movement along the chip on the streamline. Although the nanoparticles seem to have penetrated into the tumor by passing through the microchannels, they couldn't reach at the center of the tumor due to mechanical design of the tumor-on-a-chip was drawn angled.

However, while the COMSOL Multiphysics software program allows to change the size of the nanoparticle, it does not show this change visually in the simulation. Because of that in the present tumor-on-a-chip design nanoparticle size differentiation could not be observed at the end of the simulation. Moreover, the software program also does not allow to change nanoparticle shape when adjusting "Particle Tracing for Fluid Flow" physics settings.

To summarize, it was taken a goal which is design and simulate competent organ-on-a-chip systems for testing nanomaterials in all these studies. As the first step, it was decided to choose the organ that can be seen as relevant. The mechanical design of the organ was made considering the physiological state of the organ in the body. Afterwards, the system to be simulated is transferred to the simulation software program and the relevant physics are selected. Input and output are determined on the design for the relevant physics. From the Settings tab, the relevant parameters of the fluid to be sent to the system are entered. The parameters that are desired to run the simulation with or without time dependency are determined. When the simulation is completed by the program, it is possible to observe the velocity, pressure, etc. analyzes of the system. The project was formatted around these outlines.

The first organ chosen was the vessels that surround the entire body. It was foreseen that the vascular structure would be used in every organ-on-a-chip systems, and basic microflow visuals were provided on these models. On vessel-on-a-chip modeling, factors that can affect an organ-on-a-chip by minor differences in mechanical design that can be ignored were evaluated: such as shear stress. In the continuation, vascular occlusion-on-a-chip modeling was evaluated. Critical point of the vascular occlusion modeling was

instantaneous increase and decrease due to vasoconstricton. Additively, nanoparticle tracing was applied on the double-sided occlusion microfluidic chip model. It has been concluded that structures called SA-NPs can be used for nanomaterials to be effective at points where shear stress increases due to drag force in treatment models that need to be applied to eliminate vascular occlusions.

The liver, which is an organ that has been widely studied among organ-on-a-chip studies in the literature, was the second subject of the current study. In the liver-on-a-chip design, which consists of three separate steps in total, it was mentioned where the nanomaterial should be sent on the chip as the first tab. The nanomaterial can be introduced on the chip with normal flow channel, or it can be given from different channels to exhibit homogeneous distribution on the chip. In the second step of the Liver-on-a-chip design, there is a mechanical design in order to completely mix the flow defined from the different channel in the first stage at a certain concentration with the flow sent from the main channel. This design is provided by a series of extensions on the sides of the main channel. The extensions achieved a homogeneous mixture at the end of the channel. As the last step in this time-dependent liver-on-a-chip simulation, the main chip, on which cells can be planted, was created at the end of the mixing mechanism. It was reported that transmission was carried out with 4 different channels in order to distribute the flow evenly on the main chip, and the boundary condition around the wells in the main chip should be considered.

Cancer-on-a-chip designs, one of the trend organ-on-a-chip study topics, were selected and evaluated as the final subject of the present study. First, simulation was performed on *in vitro* tumor spheroid formations, which are easily created and evaluated in laboratories for cancer studies. At this point, the hydrophobicity of the materials used in organ-on-a-chip designs was evaluated. It was concluded that hydrophilic surfaces may be preferred for possible nanoparticle treatments to be defined for tumor spheroids formed on different surfaces depending on hydrophobicity, so that they can penetrate into the spheroid. A multi-channel tumor-on-a-chip design was performed considering the tumor physiology in the body. In this design, nanoparticle transmission was carried out by

making use of the EPR effect. The frequency of the channels proved to be effective for the particle to reach the tumor center.

It is possible to say for each whole design and all other small organ-on-a-chip designs in all microfluidic system designs: In order to test nanomaterials, within the scope of basic laminar flow rules, possible scenarios (especially the mechanical designs of organ-on-a-chips) such as the type of materials, their concentration, the flow rate of the fluid and its driving force to be sent to the system, the size and density of the nanomaterial, mixing mechanisms, etc. were discussed in the study. As a result of the inferences for each chip system, any situation that makes it possible to evaluate nanomaterials on organ-on-a-chip will shed light on future studies. In order for *in vitro* studies to converge to *in vivo* studies systematically, the design processes need to be detailed. In order to mimic the microenvironment in which the cells are in their normal physiology, all the steps of the design must be done according to the physiology of the organ.

REFERENCES

Ahadian, S., Civitarese, R., Bannerman, D., Mohammadi, M. H., Lu, R., Wang, E., . . . Zhao, Y. 2018. Organ- on- a- chip platforms: a convergence of advanced materials, cells, and microscale technologies. *Advanced healthcare materials, 7*(2), 1700506.

Balagaddé, F. K., You, L., Hansen, C. L., Arnold, F. H., & Quake, S. R. 2005. Long-term monitoring of bacteria undergoing programmed population control in a microchemostat. *Science, 309*(5731), 137-140.

Beebe, D. J., Mensing, G. A., & Walker, G. M. 2002. Physics and applications of microfluidics in biology. *Annual review of biomedical engineering, 4*(1), 261-286.

Bhise, N. S., Gray, R. S., Sunshine, J. C., Htet, S., Ewald, A. J., & Green, J. J. 2010. The relationship between terminal functionalization and molecular weight of a gene delivery polymer and transfection efficacy in mammary epithelial 2-D cultures and 3-D organotypic cultures. *Biomaterials, 31*(31), 8088-8096.

Burillon, C., Huot, L., Justin, V., Nataf, S., Chapuis, F., Decullier, E., & Damour, O. 2012. Cultured autologous oral mucosal epithelial cell sheet (CAOMECS) transplantation for the treatment of corneal limbal epithelial stem cell deficiency. *Investigative ophthalmology & visual science, 53*(3), 1325-1331.

Burton, A., Altman, D. G., Royston, P., & Holder, R. L. 2006. The design of simulation studies in medical statistics. *Statistics in medicine, 25*(24), 4279-4292.

Carrilho, E., Martinez, A. W., & Whitesides, G. M. 2009. Understanding wax printing: a simple micropatterning process for paper-based microfluidics. *Analytical chemistry, 81*(16), 7091-7095.

Demir, E. 2021. A review on nanotoxicity and nanogenotoxicity of different shapes of nanomaterials. *Journal of Applied Toxicology, 41*(1), 118-147.

DiMasi, J. A., Grabowski, H. G., & Hansen, R. W. 2016. Innovation in the pharmaceutical industry: new estimates of R&D costs. *Journal of health economics, 47*, 20-33.

Drewitz, M., Helbling, M., Fried, N., Bieri, M., Moritz, W., Lichtenberg, J., & Kelm, J. M. 2011. *Towards automated production and drug sensitivity testing using scaffold‐free spherical tumor microtissues* (1860-6768). Retrieved from

Duffy, D. C., McDonald, J. C., Schueller, O. J., & Whitesides, G. M. 1998. Rapid prototyping of microfluidic systems in poly (dimethylsiloxane). *Analytical chemistry, 70*(23), 4974-4984.

Egolf, P. W., & Hutter, K. 2020. *Nonlinear, Nonlocal and Fractional Turbulence: Alternative Recipes for the Modeling of Turbulence*: Springer Nature.

Fang, J., Nakamura, H., & Maeda, H. 2011. The EPR effect: unique features of tumor blood vessels for drug delivery, factors involved, and limitations and augmentation of the effect. *Advanced drug delivery reviews, 63*(3), 136-151.

Fennema, E., Rivron, N., Rouwkema, J., van Blitterswijk, C., & De Boer, J. 2013. Spheroid culture as a tool for creating 3D complex tissues. *Trends in biotechnology, 31*(2), 108-115.

Funano, S.-i., Tanaka, N., & Tanaka, Y. 2016. Vapor-based micro/nano-partitioning of fluoro-functional group immobilization for long-term stable cell patterning. *RSC advances, 6*(98), 96306-96313.

Gao, B., Jing, C., Ng, K., Pingguan-Murphy, B., & Yang, Q. 2019. Fabrication of three-dimensional islet models by the geometry-controlled hanging-drop method. *Acta Mechanica Sinica, 35*(2), 329-337.

Guillouzo, A., & Guguen-Guillouzo, C. 2008. Evolving concepts in liver tissue modeling and implications for in vitro toxicology. *Expert opinion on drug metabolism & toxicology, 4*(10), 1279-1294.

He, Q., Sudibya, H. G., Yin, Z., Wu, S., Li, H., Boey, F., . . . Zhang, H. 2010. Centimeter-long and large-scale micropatterns of reduced graphene oxide films: fabrication and sensing applications. *Acs Nano, 4*(6), 3201-3208.

Hernández-Pedro, N. Y., Rangel-López, E., Magaña-Maldonado, R., de la Cruz, V. P., Santamaría del Angel, A., Pineda, B., & Sotelo, J. 2013. Application of nanoparticles on diagnosis and therapy in gliomas. *BioMed research international, 2013*.

Inshakova, E., Inshakova, A., & Goncharov, A. 2020. *Engineered nanomaterials for energy sector: market trends, modern applications and future prospects.* Paper presented at the IOP Conference Series: Materials Science and Engineering.

Jeevanandam, J., Barhoum, A., Chan, Y. S., Dufresne, A., & Danquah, M. K. 2018. Review on nanoparticles and nanostructured materials: history, sources, toxicity and regulations. *Beilstein journal of nanotechnology, 9*(1), 1050-1074.

Kalra, A., Yetiskul, E., Wehrle, C. J., & Tuma, F. 2020. Physiology, liver. *StatPearls [Internet]*.

Kimlin, L., Kassis, J., & Virador, V. 2013. 3D in vitro tissue models and their potential for drug screening. *Expert opinion on drug discovery, 8*(12), 1455-1466.

Kirby, B. J. (2010). *Micro-and nanoscale fluid mechanics: transport in microfluidic devices*: Cambridge university press.

Knowlton, S., & Tasoglu, S. 2016. A bioprinted liver-on-a-chip for drug screening applications. *Trends in biotechnology, 34*(9), 681-682.

Kolev, N. I. 2005. Drag forces. *Multiphase Flow Dynamics 2: Thermal and Mechanical Interactions*, 27-70.

Korin, N., Kanapathipillai, M., Matthews, B. D., Crescente, M., Brill, A., Mammoto, T., . . . Bhatta, D. 2012. Shear-activated nanotherapeutics for drug targeting to obstructed blood vessels. *Science, 337*(6095), 738-742.

Kuo, C.-T., Wang, J.-Y., Lin, Y.-F., Wo, A. M., Chen, B. P., & Lee, H. 2017. Three-dimensional spheroid culture targeting versatile tissue bioassays using a PDMS-based hanging drop array. *Scientific reports, 7*(1), 1-10.

Kwak, B., Ozcelikkale, A., Shin, C. S., Park, K., & Han, B. 2014. Simulation of complex transport of nanoparticles around a tumor using tumor-microenvironment-on-chip. *Journal of Controlled Release, 194*, 157-167.

Langer, R., & Vacanti, J. P. 1993. Tissue engineering. *Science (New York, NY), 260*(5110), 920-926.

Lanza, R., Langer, R., Vacanti, J. P., & Atala, A. 2020. *Principles of tissue engineering*: Academic press.

Lee, P. J., Hung, P. J., & Lee, L. P. 2007. An artificial liver sinusoid with a microfluidic endothelial- like barrier for primary hepatocyte culture. *Biotechnology and bioengineering, 97*(5), 1340-1346.

Lee, S.-A., Kang, E., Ju, J., Kim, D.-S., & Lee, S.-H. 2013. Spheroid-based three-dimensional liver-on-a-chip to investigate hepatocyte–hepatic stellate cell interactions and flow effects. *Lab on a Chip, 13*(18), 3529-3537.

Llewellyn, S. V., Conway, G. E., Shah, U.-K., Evans, S. J., Jenkins, G. J., Clift, M. J., & Doak, S. H. 2020. Advanced 3D liver models for in vitro genotoxicity testing following long-term nanomaterial exposure. *JoVE (Journal of Visualized Experiments)*(160), e61141.

Madrid, B. B. C. L. L., & Toronto, S. S. T. Fluid Mechanics, Frank M White.

Mahto, S. K., Charwat, V., Ertl, P., Rothen-Rutishauser, B., Rhee, S. W., & Sznitman, J. 2015. Microfluidic platforms for advanced risk assessments of nanomaterials. *Nanotoxicology, 9*(3), 381-395.

Oddo, A., Morozesk, M., Lombi, E., Schmidt, T. B., Tong, Z., & Voelcker, N. H. 2021. Risk assessment on-a-chip: a cell-based microfluidic device for immunotoxicity screening. *Nanoscale Advances*.

Poon, C. 2020. Measuring the density and viscosity of culture media for optimized computational fluid dynamics analysis of in vitro devices. *bioRxiv*.

Replogle, R. L., MEISELMAN, H. J., & MERRILL, E. W. 1967. Clinical implications of blood rheology studies. *Circulation, 36*(1), 148-160.

Russell, W. M. S., & Burch, R. L. 1959. *The principles of humane experimental technique*: Methuen.

Ryu, N.-E., Lee, S.-H., & Park, H. 2019. Spheroid culture system methods and applications for mesenchymal stem cells. *Cells, 8*(12), 1620.

Sekiya, N., Matsumiya, G., Miyagawa, S., Saito, A., Shimizu, T., Okano, T., . . . Sawa, Y. 2009. Layered implantation of myoblast sheets attenuates adverse cardiac remodeling of the infarcted heart. *The Journal of thoracic and cardiovascular surgery, 138*(4), 985-993.

Shakya, K., & Chowdhury, S. R. 2019. Modelling and Simulation of Various Kinds of Blockage in Carotid Artery and Finding Their Pressure and Velocity Gradient Suitable for Measuring These Parameters Noninvasively with the Help of External Pressure and Velocity Sensors. *Sensors & Transducers, 231*(3), 15-24.

Shehab, N., Lovegrove, M. C., Geller, A. I., Rose, K. O., Weidle, N. J., & Budnitz, D. S. 2016. US emergency department visits for outpatient adverse drug events, 2013-2014. *Jama, 316*(20), 2115-2125.

Špeťuch, V., Petrík, J., Grambálová, E., Medveď, D., & Palfy, P. 2015. The Capability of The Viscosity Measurement Process. *Acta Metallurgica Slovaca, 21*(1), 53-60.

Stirland, D. L., Nichols, J. W., Miura, S., & Bae, Y. H. 2013. Mind the gap: a survey of how cancer drug carriers are susceptible to the gap between research and practice. *Journal of Controlled Release, 172*(3), 1045-1064.

Theobald, J., Ghanem, A., Wallisch, P., Banaeiyan, A. A., Andrade-Navarro, M. A., Taškova, K., . . . Reuter, S. 2018. Liver-kidney-on-chip to study toxicity of drug metabolites. *ACS Biomaterials Science & Engineering, 4*(1), 78-89.

Tiwari, M. M., & Tiwari, M. T. 2020. *ENVIRONMENTAL BEHAVIOR AND ECOTOXICITY OF ENGINEERED NANOPARTICLES TO ALGAE, PLANTS AND FUNGI.* Paper presented at the Virtual International Conference.

Viravaidya, K., Sin, A., & Shuler, M. L. 2004. Development of a microscale cell culture analog to probe naphthalene toxicity. *Biotechnology progress, 20*(1), 316-323.

Wan, L., Neumann, C., & LeDuc, P. 2020. Tumor-on-a-chip for integrating a 3D tumor microenvironment: chemical and mechanical factors. *Lab on a Chip, 20*(5), 873-888.

Wang, Z., Samanipour, R., Koo, K., & Kim, K. 2015. Organ-on-a-chip platforms for drug delivery and cell characterization: A review. *Sens. Mater, 27*(6), 487-506.

Wei, S., Yu-Qing, C., Guo-An, L., ZHANG, M., ZHANG, H.-Y., Yue-Rong, W., & Ping, H. 2016. Organs-on-chips and its applications. *Chinese Journal of Analytical Chemistry, 44*(4), 533-541.

Xia, Y., & Whitesides, G. M. 1998. Soft lithography. *Annual review of materials science*, *28*(1), 153-184.

Xiong, B., Ren, K., Shu, Y., Chen, Y., Shen, B., & Wu, H. 2014. Recent developments in microfluidics for cell studies. *Advanced materials*, *26*(31), 5525-5532.

Zhang, B., Korolj, A., Lai, B. F. L., & Radisic, M. 2018. Advances in organ-on-a-chip engineering. *Nature Reviews Materials*, *3*(8), 257-278.

Zheng, B., Tice, J. D., Roach, L. S., & Ismagilov, R. F. 2004. A droplet- based, composite PDMS/glass capillary microfluidic system for evaluating protein crystallization conditions by microbatch and vapor- diffusion methods with on- chip X- ray diffraction. *Angewandte chemie international edition*, *43*(19), 2508-2511.

Ziółkowska, K., Kwapiszewski, R., & Brzozka, Z. 2011. Microfluidic devices as tools for mimicking the in vivo environment. *New Journal of Chemistry*, *35*(5), 979-990.